Journal of Hazardous Materials 417 (2021) 125996

Contents lists available at ScienceDirect

Journal of Hazardous Materials

journal homepage: www.elsevier.com/locate/jhazmat

Exploitation of extracellular organic matter from *Micrococcus luteus* to enhance *ex situ* bioremediation of soils polluted with used lubricants

Attila Bodor [a,b], Naila Bounedjoum [a], Gábor Feigl [c], Ágnes Duzs [a,b], Krisztián Laczi [a,d], Árpád Szilágyi [a], Gábor Rákhely [a,b,*,1], Katalin Perei [a,1]

[a] Department of Biotechnology, University of Szeged, Szeged, Hungary
[b] Institute of Biophysics, Biological Research Centre, Eötvös Loránd Research Network, Szeged, Hungary
[c] Department of Plant Biology, University of Szeged, Szeged, Hungary
[d] Institute of Plant Biology, Biological Research Centre, Eötvös Loránd Research Network, Szeged, Hungary

ARTICLE INFO

Editor: Dr. R. Maria Sonia

Keywords:
EOM
Resuscitation-promoting factor
Rehabilitation
Biostimulation
Bioaugmentation
Hydrocarbon contamination
Used lubricating oil

ABSTRACT

Chronic pollution by used lubricant oils (ULOs) poses a serious challenge to the environment. Under stress conditions, microorganisms, including potential degraders, can enter a viable but non-culturable (VBNC) state, complicating the bioremediation of ULO-polluted areas. Resuscitation-promoting factors (Rpfs) can reverse this transition and/or enhance the biodegradation performance of both native and augmented strains. Here, Rpf-containing extracellular organic matter (EOM) from *Micrococcus luteus* was used to enhance the *ex situ* ULO removal in biostimulated and bioaugmented (with *Rhodococcus qingshengii* KAG C, *R. erythropolis* PR4) soils. ULO bioconversion, microbial activity, and CFUs were significantly higher in EOM-treated soils compared to corresponding control soils. After 60 days, the initial ULO concentration (52,500 mg kg^{-1}) was reduced by 37% and 45% with EOM-supplemented biostimulation and bioaugmentation, respectively. Based on high-throughput 16S rRNA analysis, the enhancement was attributable both to the reactivation of EOM-responsive hydrocarbonoclastic bacterial genera (e.g., *Pseudomonas, Comamonas, Stenotrophomonas*, *Gordonia*) and to the long-term positive effect of EOM on the degradative efficacy of the introduced rhodococci. Ecotoxicological responses revealed that reduced ULO concentration did not correlate with decreased soil toxicity. Our findings provide an insight into the applicability of EOM in bioremediation and its effects on the soil microbial activity and community composition.

1. Introduction

Lubricant oils (LOs) are produced to reduce friction and wear of machinery by forming a protective microlayer on the mechanical moving parts (Pinheiro et al., 2017b). LOs are conventionally derived from crude oil and, on average, consist of about 80–90% base oil and 10–20% chemical additives and other components (Botas et al., 2017). A wide range of application requires numerous (about 5000–10,000 different) formulations of LOs, including automotive oils, industrial oils, greases, metalworking fluids, and process oils (Mang and Gosalia, 2017). Even upon normal operation, LOs undergo various physicochemical changes, which affect their properties and cause the accumulation of harmful compounds such as combustion products, heavy metals, and polychlorinated and polyaromatic hydrocarbons (PCBs and PAHs). Europe itself consumed about 6.8 million tons of LOs in 2015, of which 50% generate waste lubricants, making used lubricant oils (ULOs) the most significant liquid hazardous waste stream in Europe (Botas et al., 2017; Pinheiro et al., 2017a). Moreover, almost 40–50% of ULOs end up in the environment as pollutants due to leakage, transportation, usage, or improper storage (Luther, 2017). Aside from the hazardous effects on human health, ULO emission also imperils the natural environment by hindering oxygen exchange on the water surface in aquatic systems or by changing the physicochemical properties of soils. The presence of lubricants, which clog pores and strongly bind to soil particles, potentially reduces water infiltration and aeration by limiting the permeability of the soil, changes the distribution of soil organic matter (SOM) and inorganic macronutrients, and ultimately disrupts the proper functioning of terrestrial ecosystems (Bodor et al., 2020b; Nowak et al., 2019).

A great variety of physicochemical approaches have been developed

* Corresponding author at: Department of Biotechnology, University of Szeged, Közép fasor 52, H-6726 Szeged, Hungary.
E-mail address: rakhely@brc.hu (G. Rákhely).
[1] These authors contributed equally to the manuscript.

https://doi.org/10.1016/j.jhazmat.2021.125996
Received 1 March 2021; Received in revised form 22 April 2021; Accepted 23 April 2021
Available online 6 May 2021

to decontaminate soils polluted with petroleum products; however, they can be expensive and destructive to treated soil matrices. Alternatively, biological treatments demonstrate strong potential, since they offer more cost efficient, environmentally sound, and sustainable techniques (Ossai et al., 2020; Sales da Silva et al., 2020). As such, bioremediation utilizes the natural degradative capability of living organisms to remove and neutralize contaminants either *in situ* (at the contaminated site) or *ex situ* (on excavated samples) (Ossai et al., 2020; Ławniczak et al., 2020). Biostimulation involves the addition of limiting nutrients to polluted environments in order to stimulate the growth of the native microbiota and accelerate its natural biodegradation processes. Bioaugmentation refers to an approach in which auto- or allochthonous microbial degraders are inoculated into contaminated sites (Ossai et al., 2020; Sales da Silva et al., 2020; Ławniczak et al., 2020). Both bioremediation procedures are promising and widely used, but the capacity and advantages of bioaugmentation remain controversial (Bodor et al., 2020b; Ławniczak et al., 2020). Introduced degraders often underperform on a field scale compared with the case under laboratory conditions due to their inability to cope with various environmental stressors (e.g., competition, predation, temperature, aeration, nutrient starvation, moisture, etc.), leading to their poor survival or transition into a zero/low-activity (viable but non-culturable: VBNC) state (Bodor et al., 2020a; Pacwa-Płociniczak et al., 2019; Su et al., 2015b).

Most bacteria naturally exist in a VBNC state, which is a subsistence-serving adaptive physiological stage in response to adverse environmental conditions, including, but not limited to, oligotrophic nutrients, extreme temperature, salinity, pH changes, and exposure to heavy metals or organic pollutants (Bodor et al., 2020a; Dong et al., 2020). Resuscitation-promoting factor (Rpf), a small cytokine-like extracellular protein, was first identified in *Micrococcus luteus* and shown to promote the resuscitation and growth of numerous Gram-positive and Gram-negative VBNC bacteria, even at picomolar concentration. Rpf-mediated resuscitation of VBNC cells is presumably based on the muralytic activity of Rpf protein (Bodor et al., 2020a). Rpf-responsive genera, such as *Rhodococcus*, *Arthrobacter*, *Bacillus*, *Mycobacterium*, *Leifsonia*, *Nocardia*, *Olivibacter*, *Bacillus*, *Streptomyces*, and *Novosphingobium*, include well-known degraders (Bodor et al., 2020a; Bounedjoum et al., 2018; Cai et al., 2020a; Ye et al., 2020). Moreover, recent studies have revealed other Rpf-responsive populations with potential functions of environmental remediation in the phyla *Proteobacteria*, *Bacteriodetes*, and *Actinobacteria* (Su et al., 2019a,b; Yu et al., 2020). Several VBNC bacteria, recovered by Rpf supplementation, showed the ability to degrade phenol, biphenyls, cellulose, and dyes and/or remove nitrogen (Bodor et al., 2020a; Su et al., 2019a,c), while Rpf treatment enhanced the removal of such compounds in contaminated samples (Bodor et al., 2020a; Bounedjoum et al., 2018). Rpf represents the dominant protein component in the sterile filtered culture supernatant of *M. luteus,* actively growing on lactate minimal medium. This fermentation broth is often referred to as extracellular organic matter (EOM) or supernatant Rpf (SRpf) (Bodor et al., 2020a). Compared with the use of purified recombinant Rpf, EOM possesses the advantages of containing polysaccharides and additional muralytic proteins, all potentially involved in resuscitation processes (Su et al., 2015c; Ye et al., 2020). Thus, EOM can be considered as a cost-efficient and easy-to-prepare supplement to promote the recovery of VBNC bacteria from environmental samples and enhance their ability to degrade pollutants. Despite extensive research on the resuscitation of VBNC pathogens (Dong et al., 2020), our knowledge of the resuscitation of pollutant-degraders, the potential environmental functions of VBNC bacteria in polluted environments, and the applicability of Rpf- or EOM-based bioremediation methods is still limited (Bodor et al., 2020a).

Since lubricants are less volatile and less biodegradable, there are no reports on their complete bioconversion using current methodologies. Thus, complex optimization and risk assessment are needed to deepen our understanding of the biological processes underlying (U)LO removal (Bodor et al., 2020b; Lee et al., 2007; Nowak et al., 2019). Therefore, the aim of this study was to evaluate the feasibility of EOM-stimulated bioremediation by monitoring changes in microbial activity, culturable cell counts, microbial community composition, total petrol hydrocarbon (TPH) bioconversion, and soil phytotoxicity. To this end, the *ex situ* bioremediation of a local ULO-polluted site was modeled in bench-scale soil microcosm set-ups, through conventional and EOM-supplemented biostimulation and bioaugmentation approaches. A bacterial artificial consortium, composed of *Rhodococcus qingshengii* KAG C and *Rhodococcus erythropolis* PR4, was used for bioaugmentation. To the best of our knowledge, this is the first successful attempt to use Rpf-containing EOM from *M. luteus* as a stimulatory agent to decontaminate ULO-polluted soils, and to report the effect of EOM addition on the ULO-degrading capability of not previously resuscitated or Rpf-treated, *Rhodococcus* strains.

2. Materials and methods

2.1. Chemicals

All chemicals and analytical-grade solvents were purchased from standard commercial suppliers (Reanal, Sigma-Merck, VWR International).

2.2. Soil sampling and characterization

The soil samples used in this study were obtained from Szeged, Hungary (Fig. S1), from a railway marshaling yard of MÁV Hungarian State Railways (Hungary). Soil contamination by ULOs has been a long-standing environmental problem at this location. According to the FAO classification, vertisols are prevalent in this area (Mezősi, 2017). The sampling site was described in our previous report (Bodor et al., 2020b). Formerly, the uncontaminated soil was characterized by a dark color, high organic matter content (23.5%), near-neutral pH (7.79), high water-holding capacity (47.2%), clay texture, and slight salinity (0.11%).

For this study, subsequent sampling of the ULO-polluted soil was performed 1 year later, which took place at the same contaminated site but not at the exact same locations (Fig. S1). Average soil samples (approx. 10,000 g each) were collected and handled as described by Bodor et al., 2020b. A composite soil, consisting of the six ULO-polluted average soils mixed at equal proportions, was used to construct bench-scale microcosms. SOM was estimated based on the weight loss on ignition at 550 ℃ for 4 h (Heiri et al., 2001). Total C and total N were analyzed with a Vario Max CN Analyzer (Elementar Group, Hanau, Germany) (Kakuk et al., 2017). Available P was determined in accordance with the work of Bodor et al., 2020b. Heavy metal concentration measurements were carried out by staff at the Department of Physical Geography and Geoinformatics (University of Szeged, Hungary) using an Optima 7000DV inductively coupled plasma atomic/optical emission spectrometer (ICP-OES; PerkinElmer Inc., Waltham, USA), as described by Farsang et al. (2020).

2.3. Preparation of EOM from Micrococcus luteus

Rpf-containing EOM from *Micrococcus luteus* IAM 14879 (=JCM 21373=NCIMB 13267) was prepared using a modified version of the method described by Su et al., 2015c. Starter culture was incubated in Luria Bertani (LB) broth on a rotary shaker (160 rpm, 30 ℃) until OD_{600} = 1.0 (Laczi et al., 2015). Then, cells were centrifuged (13,000 rpm, 10 min, 4 ℃) and resuspended in modified lactate minimal medium (LMM) containing 4 g L^{-1} NH_4Cl, 1.4 g L^{-1} KH_2PO_4, 0.005 g L^{-1} biotin, 0.02 g L^{-1} methionine, 0.04 g L^{-1} thiamine, 0.03 g L^{-1} $MgSO_4$, 13.6 mL of lactic acid, 1.5 mL of trace element solution (0.375 g L^{-1} $CuSO_4 \times 5 H_2O$, 0.785 g L^{-1} $MnCl_2 \times 4 H_2O$, 0.183 g L^{-1} $FeSO_4 \times 7H_2O$, 0.029 g L^{-1} $Na_2MoO_4 \times 2H_2O$, and 0.089 g L^{-1} $ZnSO_4 \times 7 H_2O$) and adjusted to pH = 7.5. Resuspended cells were inoculated (4% v v^{-1}) into fresh LMM

under the same conditions until they reached the stationary phase. The fermentation broth was centrifuged (13,000 rpm, 10 min, 4 ℃) and then the supernatant was filtered through a 0.22 μm filter to ensure the complete removal of floating cells. The obtained *M. luteus* EOM was stored at −20 ℃ for further experiments.

2.4. Bacterial strains

Rhodococcus erythropolis PR4 (NBRC 100887) and *Rhodococcus qingshengii* KAG C (DSM 111937) strains were used for bioaugmentation. *R. erythropolis* PR4 is a well-characterized hydrocarbonoclastic marine bacterium (Laczi et al., 2015; Komukai-Nakamura et al., 1996), obtained from the National Institute of Technology and Evaluation, Biological Resource Center (NBRC; Kisarazu-shi, Chiba, Japan). *R. qingshengii* KAG C was isolated from diesel oil in our laboratory. Both strains were previously reported to degrade LOs (Bodor et al., 2020b).

2.5. Bioremediation experimental design

The feasibility of different bioremediation strategies for ULO-polluted soils, including nutrient stimulation and bioaugmentation with or without the addition of EOM from *M. luteus*, was examined in bench-scale microcosm set-ups. The detailed experimental design is presented in Table 1.

For each microcosm, 10 kg of ULO-polluted composite soil (not autoclaved) was weighed into a plastic pot (volume: 13 L, height: 27 cm, width: 32 cm, depth: 27 cm) and incubated at room temperature (20–25 ℃) for 60 days. Every 2 days, during the whole incubation process, the content of each pot was thoroughly mixed to provide sufficient aeration. The experimental design included five experimental conditions: (a) natural attenuation (NA, the intrinsic degradative capability of the ULO-polluted soil), (b) biostimulation (BS, stimulation of the degradative performance of the indigenous microbiota in the ULO-polluted soil using inorganic sources of nitrogen, phosphorus, and potassium), (c) biostimulation and EOM addition (BS+EOM, enhanced biostimulation), (d) bioaugmentation combined with biostimulation (BAS, stimulated soil inoculated with hydrocarbon-degrader *Rhodococcus* strains), and (e) bioaugmentation combined with biostimulation and EOM addition (BAS+EOM, enhanced bioaugmentation). Soil moisture was maintained between 15% and 30% (approx. 30–60% of total WHC) with sterile distilled water (Lee et al., 2018; Liu et al., 2020). Without any nutrient addition, NA was considered as a control, representing the natural ability of the polluted soil to degrade ULO in its own condition. In all bioremediation treatments, the C/N/P ratio was adjusted to 500/10/1 using K_2HPO_4 and NH_4NO_3 as water-soluble sources of inorganic nitrogen, phosphorus, and potassium (NPK) (Lee et al., 2007). Additionally, both BS+EOM and BAS+EOM were supplemented with 10% Rpf-containing EOM (Su et al., 2015c) in order to stimulate or reactivate potentially functional degraders in the indigenous microbial community and to enhance the ULO-biodegradation performance of the inoculated strains. Both *R. qingshengii* KAG C and *R. erythropolis* PR4 were introduced into the augmented microcosms at inoculation levels of 2×10^7 cells g^{-1} and 2×10^7 cells g^{-1}, respectively. Both strains proved to be able to utilize diverse hydrophobic contaminants as sole carbon and energy sources, including LOs (Bodor et al., 2020b; Laczi et al., 2015). Starter cultures and inocula were prepared in accordance with the work of Laczi et al. (2015).

During the experiment, each microcosm was sampled at three distinct points of the pot, using a sterile coring tool, which cuts a vertical soil section of 20 mm in diameter from the top to the bottom of the pot. Column soil samples were collected at 0, 5, 10, 15, 20, 30, and 60 days. Then, each column was homogenized and further analyzed for the determination of TPH, microbial activity, cell count, and soil enzyme activity. A total of 95 samples were included in the analysis of microbial community composition. (To map the changes in the soil microbiome in detail during the first incubation period and at the end of the experiment, all triplicates were used on days 0, 5, 10, 15, and 60; however, one of the triplicates was discarded on days 20 and 30.).

Table 1
Microcosm experimental setup. In each case, 10 kg ULO[a]-contaminated soil was treated and the soil moisture was adjusted to 30%.

Treatment	Supplemented components	Aim of treatment
NA	nothing	natural attenuation
BS	+ NPK[b] (C/N/P=500/10/1)	biostimulation
BS+EOM[c]	+ NPK (C/N/P≈500/10/1) + 10% EOM	biostimulation+EOM
BAS	+ NPK (C/N/P=500/10/1) + 2x10^7 CFU g^{-1} *R. qingshengii* KAG C + 2x10^7 CFU g^{-1} *R. erythropolis* PR4	bioaugmentation+biostimulation
BAS+EOM	+ NPK (C/N/P≈500/10/1) + 2x10^7 CFU g^{-1} *R. qingshengii* KAG C + 2x10^7 CFU g^{-1} *R. erythropolis* PR4 + 10% EOM	bioaugmentation+biostimulation+EOM

[a] ULO: Used lubricant oil
[b] NPK: Fertilization with inorganic nitrogen (N), phosphorus (P), and potassium (K)
[c] EOM: Extracellular organic matter from *Micrococcus luteus*

2.6. TPH determination and removal

Residual TPH concentrations in each soil microcosm were quantified based on the procedure of Tsuboi et al. (2015) with minor modifications: 1 g of homogenized soil sample (previously dried at 105 ℃) was extracted using 10 mL of carbon disulfide as a solvent (Barwick et al., 1998) and shaken vigorously for 1 h. Afterwards, the soil extract was centrifuged (13,000 rpm, 3 min) to separate soil particles from the liquid phase and analyzed with an Infracal TOG/TPH Analyzer CVH-1 (Wilks Enterprise Inc., Norwalk, USA) instrument. TPH concentrations were expressed as mg kg^{-1} per dry soil weight.

TPH removal efficiency was calculated using Eq. (1):

$$\text{Bioconversion } (\%) = [(C_0 - C_e)/C_0] \cdot 100, \quad (1)$$

where C_0 and C_e represent initial TPH concentration in the soil microcosm and TPH concentration in the soil microcosm at the end of the incubation period, respectively.

2.7. Decay rate calculation

TPH decay rate was approximated applying the first-order Eq. (2) (Wang et al., 2016):

$$C_e = C_0 \exp(-kt), \quad (2)$$

where C_0, C_e, k, and t represent initial TPH concentration in the soil microcosm (mg kg^{-1}), TPH concentration in the soil microcosm at the end of the incubation period (mg kg^{-1}), decay rate (day^{-1}), and incubation time (days), respectively.

2.8. Microbial respiration monitoring

Microbial respiration activity (RA) was measured using a Shimadzu GC-2010 gas chromatograph (Shimadzu Corp., Kyoto, Japan) with the operation parameters previously detailed by Bodor et al., 2020b. For RA, soil samples (6 g) from each microcosm were collected, sealed into 125

mL serum vials (Merck KGaA, Darmstadt, Germany), and then incubated in the dark at 25 ℃ for 10 days. Every 2 days, the vials were opened under sterile conditions and their headspaces were refreshed. All vials were discarded after 10 days and a new set of vials, containing soils freshly sampled from each microcosm, was incubated for further respiration monitoring. This process was repeated throughout the whole experiment in order to characterize RA in microcosms as accurately as possible. Results were determined on a cumulative basis of mg of CO_2 g^{-1} soil and mg CO_2 g^{-1} soil 48 h^{-1}.

2.9. Microbial enumeration

Aerobic heterotrophic bacterial counts (AHBs) were determined using a modified version of the method reported by Wu et al. (2017). Homogenized soil samples (5 g) were suspended in 10 mL of 0.9% (w v^{-1}) sterile saline solution and shaken for 30 min. Subsequent serial dilutions of each soil suspension were plated on LB agar media (Kis et al., 2015) and colony-forming units (CFUs) were enumerated after 3 days of incubation at 25 ℃. Results are expressed as logCFU g^{-1} per dry soil weight.

2.10. Determination of soil enzyme activity

The activity of catalase (CAT) was assayed in accordance with a titrimetric method (Stepniewska et al., 2009). A total of 40 mL of distilled water and 5 mL of 0.3% (w w^{-1}) H_2O_2 solution were added to each soil sample (2 g) from the microcosms. After 20 min of shaking, 5 mL of 1.5 M H_2SO_4 was added. Then, the suspension was filtrated and the residual H_2O_2 was back-titrated with 0.02 M $KMnO_4$. Catalase activity was expressed using the reacting amount of permanganate calculated per dry soil weight. Soil samples without H_2O_2 addition were used as blanks.

Dehydrogenase (DH) activity was determined by a procedure (Wolińska et al., 2016) based on reducing 2,3,5-triphenyltetrazolium chloride (TTC). Soil samples (6 g) from each microcosm were mixed with 0.12 g of $CaCO_3$, 4 mL of distilled water, and 1 mL of 3% (w v^{-1}) TTC solution, and then incubated for 20 h at 30 ℃. Afterwards, samples were extracted with 25 mL of ethanol for 1 h in the dark and the absorption of filtered extracts was measured at 485 nm. Results are presented as micrograms of produced triphenylformazan (TPF) per dry soil weight.

2.11. DNA extraction, amplification, and Illumina MiSeq sequencing

QIAGEN DNeasy® PowerSoil® Kit (QIAGEN GmbH, Hilden, Germany) was used for the isolation of total microbial DNA from homogenized column soil samples (250 mg), following the manufacturer's instructions. PCR amplification of the V3–V4 regions of the 16S rRNA gene (95 ℃ for 3 min; followed by 25 cycles at 95 ℃ for 30 s, 55 ℃ for 30 s, and 72 ℃ for 30 s; and final extension at 72 ℃ for 5 min, followed by cooling to 4 ℃) was performed using recommended Illumina 16S 341 F forward and Illumina 16S 805R reverse primers (Zheng et al., 2015), in accordance with the Illumina protocol (Illumina, San Diego, CA, USA). PCR reaction mixtures (25 μL) contained 12.5 μL of 2 × KAPA HiFi HotStart Ready Mix, 5 μL of each primer (1 μM), and 2.5 μL of genomic DNA template (5 ng μL^{-1}). The resulting V3–V4 16S rRNA amplicons were purified using AMPure XP beads. Both paired-end library preparation, using NEBNext® Ultra™ II DNA Library Prep Kit for Illumina, and DNA sequencing, carried out on the Illumina MiSeq platform (Illumina Inc., San Diego, CA, USA) using Illumina MiSeq® Reagent Kit v2 with 500 cycles, were outsourced to Seqomics Ltd. (Mórahalom, Hungary). A total of 6048,278 reads across 95 libraries were obtained following paired-end merging.

2.12. Bioinformatic analyses

Raw sequences from the V3–V4 16S rRNA gene region were imported into Qiime 2 (Quantitative Insights into Microbial Ecology 2) version 2020.2 (Bolyen et al., 2019). Sequence pairs were merged with the Qiime 2 VSEARCH plugin (Rognes et al., 2016). After dereplication, operational taxonomic units (OTUs) were clustered at 97% similarity with VSEARCH and then filtered for total frequency of 0.005% as a lower cut-off. OTUs were classified with the Qiime 2 scikit-learn plugin (Pedregosa et al., 2011). The SILVA 138 16S database trained with standard Illumina 16S V3-V4 primers (forward: 5′-CCTACGGGNGGCWGCAG-3′, reverse: 5′-GACTACHVGGGTATCTAATCC-3′) was used for classification (Quast et al., 2013). Qiime 2 was applied to calculate microbial diversity within a community (alpha diversity) and perform principal coordinate analysis (PCoA) to visualize differences in microbial diversity between samples (beta diversity). A Venn diagram was generated using the Bioinformatics & Evolutionary Genomics webtool (http://bioinformatics.psb.ugent.be/webtools/Venn), while heatmap plots were created in Microsoft Excel 2016.

2.13. Soil phytotoxicity tests

Modified seed germination tests, based on the method of Poi et al. (2017), were conducted at the beginning and end of the 60-day-long bioremediation experiments in order to assess changes in soil conditions following the various treatments. To this end, 10 g (wet weight) of test soil was weighed into a sterile Petri dish with a diameter of 60 mm, and a total of 20 Indian mustard seeds (*Brassica juncea* L. Czern. Var. "Negro Caballo") were placed and equally distributed on the soil surface. An aliquot of 2 mL of distilled water was evenly added onto the soil samples. Afterwards, each Petri dish was closed but not sealed, and *Brassica* seeds were left to germinate for 4 days at 25 ℃ in the dark. Seeds with visible roots after 4 days were counted as germinated. Root lengths were measured from the transition points among the hypocotyl to their extremities. Finally, relative seed germination and relative root length values were used to calculate the germination index applying Eq. (3) (Nwankwegu et al., 2016):

$$\text{Index of germination (IG\%)} = [(\%\ \text{seed germination})\cdot(\%\ \text{root length})]/100 \quad (3)$$

In all cases, the uncontaminated soil sample, taken in the near vicinity of the polluted site, was used as a control.

2.14. Microscopic analysis of the root apical meristem cells

The vitality and membrane integrity of the root apical meristem cells of *Brassica* seedlings (grown as detailed in Section 2.12) were determined in accordance with the methods of Feigl et al. (2016) and Nair and Chung, 2017, respectively, with slight modifications. After being washed in distilled water, approx. 10-mm-long root tip segments were cut and incubated in 2 mL of dye/buffer solutions in Petri dishes with a diameter of 2 cm at room temperature in the dark. A total of 10 μM fluorescein diacetate (FDA) solution (in 10/50 mM MES/KCl buffer, pH = 6.15) and 3 μg mL^{-1} propidium iodide (PI) solution (in distilled water) were used to counterstain viable and dead cells of the root meristem, respectively. Following the staining procedure (25 min for FDA and 1 min for PI), root samples were placed onto microscopic slides and investigated under a Zeiss Axiovert 200 M inverted microscope (Carl Zeiss, Jena, Germany) equipped with filter set 10 (exc.: 450–490, em.: 515–565 nm) for FDA and filter set 20HE (exc.: 546/12, em.: 607/80) for PI. The fluorescence intensity of root meristem cells was evaluated on digital photographs (taken by Axiocam HR, HQ CCD) using Axiovision Rel. 4.8 software within circles with a radius of 100 μm.

2.15. Statistical analysis

The data obtained in this study are expressed as the mean values with

their standard errors. Multiple comparison analyses were performed with SigmaPlot 11.0 software (Systat Software Inc., Erkrath, Germany) using one-way analysis of variance (ANOVA) and Duncan's multiple range test at the significance level of 5%.

3. Results and discussion

3.1. Chemical and microbiological properties of the polluted soil

The TPH concentration in the six ULO-polluted soil samples ranged from 20,800 mg kg^{-1} to 115,100 mg kg^{-1} (Fig. S1). Selected chemical and microbiological parameters of the composite soil, constructed from these six ULO-polluted soil samples, are presented in Table S1. These results are in line with the data from our previous soil sampling (Bodor et al., 2020b). Despite the high level of hydrocarbon contamination (52, 500 mg TPH kg^{-1} soil) and the presence of several heavy metals, a considerable number of culturable aerobic heterotrophic bacteria were detected (7.1 logCFU g^{-1} soil). SOM (22.4%) and total carbon content (180.5 g kg^{-1} soil) were high, which are in line with the elevated concentrations of petroleum hydrocarbons. The C/N/P ratio was 512/10/0.05. An increased ratio of C and N is often observed in oil-contaminated soil due to the small number of hydrocarbon pollutants with nitrogenous moieties (Gałązka et al., 2018). Although a C/N/P ratio of 100/10/(1−5) is generally considered to be optimal for bioremediation operations in soil (Grace Liu et al., 2011; Wu et al., 2016), Lee et al. (2007) found a C/N/P ratio of 500/10/1 to be more effective at accelerating the biodegradation of waste lubricants. These parameters suggested that the supplementation of an appropriate amount of NPK nutrients could impact the cell counts of potential degraders in ULO-contaminated composite soil, leading to the enhanced bioconversion of ULOs.

3.2. Soil microcosm experiments

3.2.1. EOM effect on hydrocarbon removal

Our objective was to compare the hydrocarbon biodegradation performance of the conventional and EOM-supplemented biostimulation and bioaugmentation approaches. Fig. 1A shows the soil TPH concentrations throughout the whole experiment. After 60 days, initial TPH content was reduced from 52,500 mg kg^{-1} to a value ranging from 44,400 to 29,800 mg kg^{-1}. Generally, a two-phase degradation pattern was observed in all microcosms. A clear decrease in soil TPH levels during the first 20 days of incubation was followed by a plateau. According to the literature, the selective biodegradation of easily degradable and accessible hydrocarbons can lead to an increased proportion of hazardous persistent hydrocarbon fractions. Moreover, in some cases, the incomplete microbial degradation can result in intermediates or breakdown products, which are more toxic than the original contaminant (Montagnolli et al., 2015; Khan et al., 2018). The aging process of hydrocarbon contamination in soil causes decreased availability of the contaminants (Koshlaf and Ball, 2017). Their mobility, however, can be increased by bacterial surfactants. Most of the hydrocarbonoclastic bacteria (including the inoculated *Rhodococcus* strains) are able to produce surface-attached or extracellular biosurfactants in order to increase the bioavailability of the hydrophobic substrate (Khan et al., 2018; Varjani and Upasani, 2017). In this study, nutrient and water contents were monitored and sustained throughout the whole incubation period; therefore, the apparent limitation of microbial capacity for hydrocarbon removal in the second stage of bioremediation was presumably due to the depletion of easily degradable and accessible hydrocarbon fractions, the release of toxic by-products from ULO biodegradation, the increased bioavailability of hazardous ULO components induced by bacterial surface-active compounds, or any combination of these molecular events (Pacwa-Płociniczak et al., 2019; Bekins et al., 2020; Wei et al., 2020).

TPH bioconversion yields were determined at the end of the two biodegradation stages (Fig. 2 and Table 2). Compared with the slight ULO removal (9%) observed in NA (water treatment only) after 20 days, biostimulation treatment (BS) and the inoculation of *R. qingshengii* KAG C and *R. erytropolis* PR4 strains (BAS) significantly improved the TPH bioconversion to 22% and 24%, respectively. Nevertheless, ANOVA showed no significant difference between BS and BAS. EOM-supplemented microcosms started to deplete TPH levels with a delay (Fig. 1A), supposedly due to the preferred consumption of the easily available carbon sources in EOM by actively growing bacteria. Rpf is the main protein component in EOM, while its polysaccharide content might be dominated by cell wall fragments released by the muralytic activity of Rpf (the monosaccharide content of EOM was at the detection limit). This activity is generally considered to be responsible for the Rpf-mediated resuscitation of VBNC bacteria (Bodor et al., 2020a; Su et al., 2015c). We supposed that during the initial delay of EOM-supplemented microcosms in TPH reduction, Rpf reactivated potentially functional hydrocarbonoclastic bacterial taxa (this claim was later supported by metagenomics). Consequently, BS+EOM (37%) and BAS+EOM (43%) were found to be the most effective in ULO bioconversion by the end of the first bioremediation phase (Fig. 2A). Considering the whole 60 days of treatment, the ranking for the overall TPH bioconversion is as follows: BAS+EOM > BS+EOM > BAS > BS > NA, with percentages of 45%, 37%, 35%, 30%, and 19%, respectively (Fig. 2B and Table 2). Only few reports are available on the Rpf- or EOM-facilitated bioremediation, and most of them are focusing on the enhanced biodegradation of PCBs, phenol, or textile dyes in aquatic systems (Bodor et al., 2020a). In contrast, we demonstrated the first EOM-enhanced bioconversion of persistent ULOs in such a complex environment as an aged contaminated soil.

It should be noted that although BAS+EOM and BS+EOM achieved the highest ULO removal throughout the whole incubation, the majority of the biodegradation took place in the first 20 days, implying a limited time positive effect of EOM. From the comparison of first-stage TPH bioconversions detected in BAS+EOM, BAS, and BS+EOM, it can be inferred that the increased hydrocarbon removal of BAS+EOM was likely due to the accelerated microbial activity of autochthonous degraders (including the resuscitated taxa) and not due to the introduced rhodococci. The lack of significant differences between BAS and BS, or between their EOM-supplemented counterparts, further supports the capacity limit of allochthonous bioaugmentation (Ławniczak et al., 2020). This is especially the case in aged petroleum-contaminated soils, where exogenous strains are often unable to over perform or compete with the native microbiota, which has already acclimated to contaminated conditions (Bodor et al., 2020b). The presence of indigenous degraders explains the ULO bioconversions observed in NA, BS, and BS+EOM, demonstrating that their TPH biodegradation performance can be effectively accelerated by adequate soil moisture (Lee et al., 2018) or stimulating treatments, including NPK (Lee et al., 2007; Malina and Zawierucha, 2007) or EOM supplementation. In contrast to the early-phase EOM effect, which mainly stimulated the autochthonous microbiota, the second-phase BAS+EOM results suggest that EOM might have a long-term positive effect on the biodegradation performance of the introduced *Rhodococcus* strains. Similar results were reported by Ye and colleagues (Ye et al., 2020) about the Rpf-accelerated PCB removal of *Rhodococcus biphenylivorans* $TG9^T$ in soil microcosms. *R. biphenylivorans* $TG9^T$, however, was isolated by exploiting the resuscitation effect of Rpf (Su et al., 2015a), while *R. qingshengii* KAG C and *R. erythropolis* PR4 were not Rpf-treated before. Therefore; in contrast to previous reports, our results demonstrated that Rpf-containing EOM was even able to enhance the biodegradation performance of previously not resuscitated bacteria.

A first-order kinetic model assumes an exponential decay pattern with an asymptote to zero, whereas the rate of substrate decay is directly proportional to the substrate concentration (Lee et al., 2007). Although these conditions are not properly met in the case of TPH biodegradation, a tremendous amount of empirical data indicate that the fate of

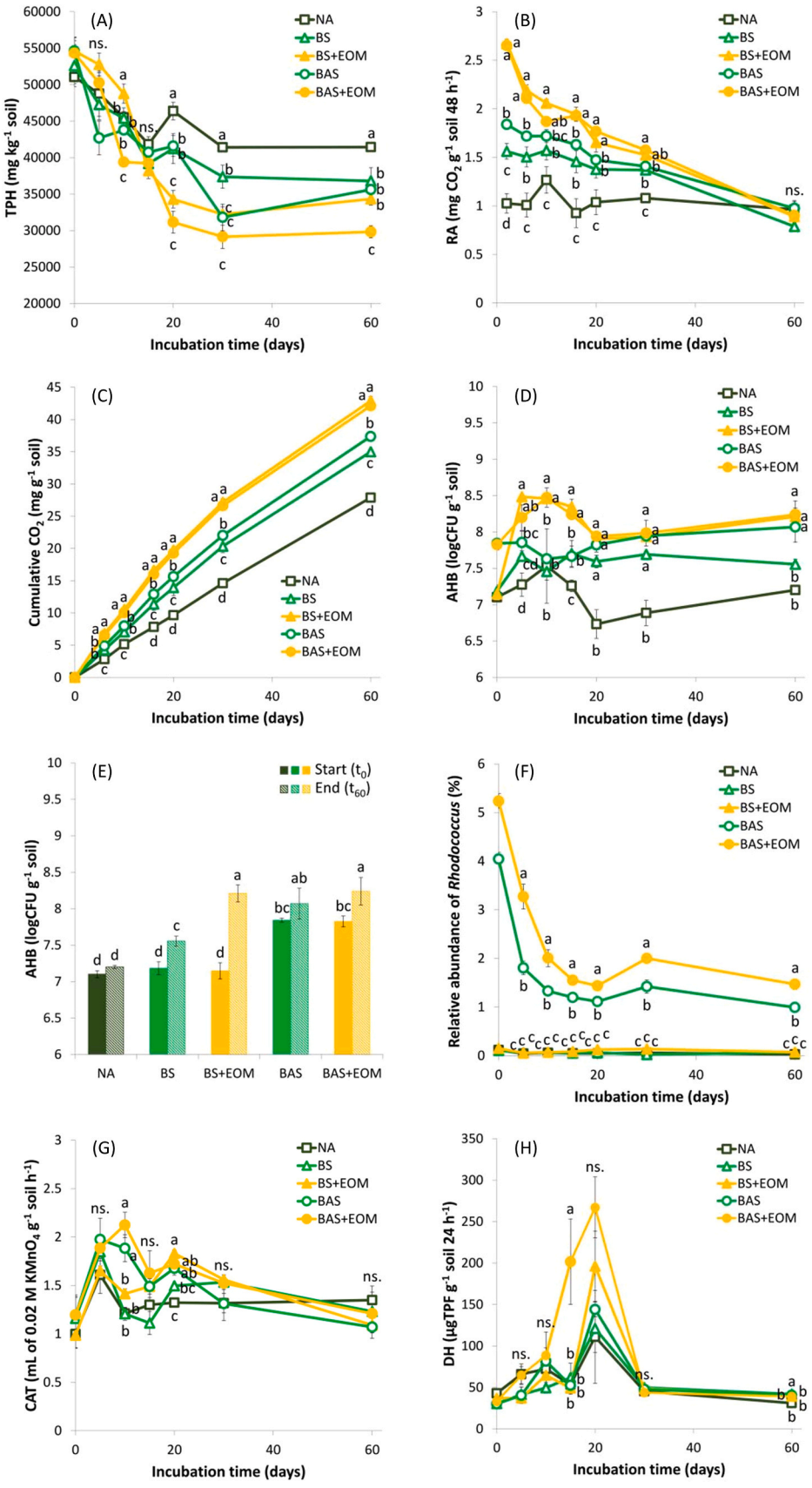

Fig. 1. (A) TPH degradation profile; (B) changes in soil respiration activity (RA); (C) cumulative CO_2 evolution; (D) changes in the number of cultivable aerobic heterotrophic bacteria (AHB); (E) AHB cell counts at the onset (t_0) and after 60 days (t_{60}) in each soil microcosm; (F) changes in the relative abundance of the genus *Rhodococcus*; (G) changes in catalase (CAT) activity; and (H) changes in dehydrogenase (DH) activity in soil microcosms over 60 days. Different letters in the same remediation time or over the bars represent a statistically significant difference at $p \leq 0.05$ ($n \geq 3$ except for days 20 and 30 of the relative abundances, where $n = 2$).

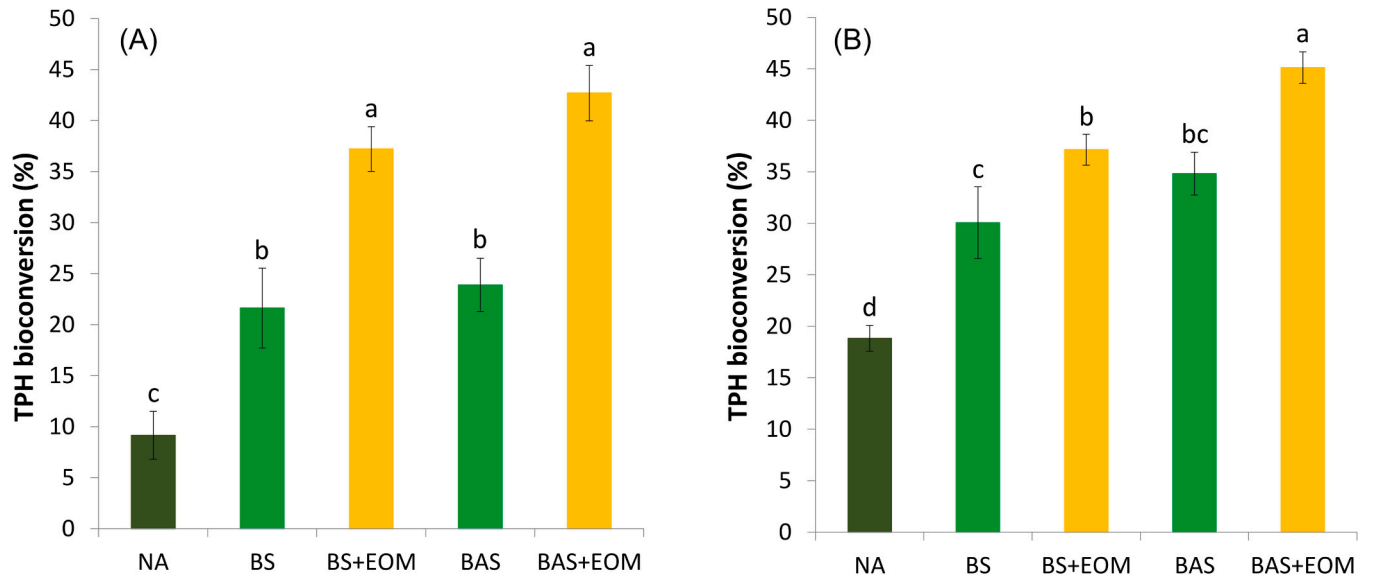

Fig. 2. Bioconversion of total petrol hydrocarbons (TPH) in soil microcosms (A) after 20 days and (B) after 60 days of incubation. Different letters in the same remediation time represent a statistically significant difference at $p \leq 0.05$ ($n = 6$).

Table 2
Percentage of TPH removal and calculated first-order decay rate for each soil microcosm.

Treatment	NA	BS	BS+EOM	BAS	BAS+EOM
First decay period (from day 0 to day 20)[a]					
TPH removal (%)[b]	9	22	37	24	43
Decay rate (day^{-1})[c]	0.003	0.008	0.016	0.009	0.019
Second decay period (from day 20 to day 60)[d]					
TPH removal (%)	10	8	0	11	2
Decay rate (day^{-1})	0.001	0.001	0	0.002	0.001
Decay period (from day 0 to day 60)[e]					
TPH removal (%)	19	30	37	35	45
Decay rate (day^{-1})	0.002	0.004	0.005	0.005	0.007

[a] Incubation period from the start (day 0) to the day that the TPH bioconversion trend leveled off (day 20).
[b] Equation (1) in text.
[c] Equation (2) in text.
[d] Incubation period from the beginning of the second step of TPH bioconversion (day 20) to the end of the experiment.
[e] The whole incubation period (60 days) was used for the calculation of decay rate.

hydrocarbon contamination in the soil can be easily anticipated and predicted by applying first-order approximation (Lee et al., 2007; Wang et al., 2016; Agarry et al., 2013). For the sake of simplicity of the data analysis, we used first-order kinetics to calculate the decay rates of ULOs, despite its above-mentioned limitations. Owing to the biphasic TPH degradation profile, a single decay rate would not describe the biodegradation kinetics properly; hence, decay rates were also defined according to the breakpoint observed around 20 days in order to characterize the early and late phases of ULO biodegradation (Table 2). In the first degradation period (before the TPH bioconversion leveled off), the decay rates of the EOM-supplemented BAS+EOM and BS+EOM were 0.019 day^{-1} and 0.016 day^{-1}, respectively, while the decay rates of the conventional bioremediation approaches were comparably lower with values of 0.009 day^{-1}, 0.008 day^{-1}, and 0.003 day^{-1} for BAS, BS, and NA, respectively. The ULO contamination of our study soil was the consequence of long-term pollution. Thus, weathering of the contamination, together with the primary bioconversion of the lighter, easily biodegradable ULO fractions, could lead to limited bioavailability or to the accumulation of toxic compounds (Pacwa-Płociniczak et al., 2019; Suja et al., 2014). Both phenomena can provide an explanation for the flattened bioconversion trends after 20 days. In the second degradation period, decay rates decreased to 0.001, 0, 0.002, 0.001, and 0.001 day^{-1} in BAS+EOM, BS+EOM, BAS, BS, and NA, respectively, highlighting the importance of avoiding the exclusive use of early phase or absolute kinetic data to predict the later fate of hydrocarbons in contaminated soils (Lee et al., 2007).

From these data, we concluded that EOM supplementation might be effectively applied to accelerate the early-phase ULO removal by the local microbial community, and to enhance the overall biodegradation performance of the augmented rhodococci.

3.2.2. *Microbial activity and cell counts during biodegradation*

Since the microbial mineralization of organic compounds results in the evolution of CO_2 as a by-product, CO_2 production is generally considered as a measure of microbial activity (Lee et al., 2007). Based on their respiratory activities (Fig. 1B) and cumulative CO_2 evolution (Fig. 1C), all microcosms contained viable and metabolically active microbial communities. Compared with the steady RA of NA, all treatments showed higher rates of CO_2 evolution, especially at the early phase, due to the supplementation of inorganic nutrients (NPK) or the addition of exogenous degraders, both promoting ULO biodegradation. It should be noted that the dead biomass (or necromass) of non-surviving bacteria from the inoculum can provide additional carbon and energy sources for indigenous microorganisms (Pacwa-Płociniczak et al., 2019). Considering that EOM might contain additional carbon sources (Su et al., 2015c), a supplementary stimulation effect could also be responsible for the substantial increase in the initial CO_2 evolution of BS+EOM and BAS+EOM. Over time, the differences between treatments gradually disappeared, and similar respiration rates were detected in all microcosms by the end of the bioremediation experiment. Since an aged contaminated soil likely contains barely degradable hydrocarbons or those that have low bioavailability, the gradual decrease in RA was possibly due to similar reasons as given above to explain why the two-phase degradation pattern was observed in all microcosms (Pacwa-Płociniczak et al., 2019).

Both conventional and EOM-supplemented bioremediation treatments increased the initial cell counts (approx. 10^7 cells per gram) of cultivable aerobic heterotrophic bacteria (AHB) compared with NA (Fig. 1D). AHB cell counts of BS and BAS were steady and generally higher than that of NA. In the early phase, EOM addition dramatically increased AHB cell counts compared with any other treatments.

Although cultivable cell counts of BAS+EOM and BS+EOM slightly decreased by the 20th day of incubation, they remained high during the second bioremediation phase. Based on the comparison of initial AHB cell counts to those that were detected at the 60th day of incubation, EOM-supplemented microcosms showed the most significant changes (Fig. 1E).

Enzymatic activity in soil is often used as an eco-monitoring indicator of soil quality and health (Wolińska et al., 2016). An initial increase in the catalase (CAT) and dehydrogenase (DH) activities (Fig. 1G and H) can be interpreted as an indication of enhanced aerobic microbial activity and decomposition of organic compounds (Lee et al., 2007; Wu et al., 2017). BAS+EOM and BS+EOM reached almost 10-fold higher DH activities with the maximum values after 20 days. However, the early-phase boost of both enzymes, observed in all treatments, was then followed by an attenuation to the background level during the late phase of bioremediation. Our results are consistent with previous reports (Lee et al., 2007; Wolińska et al., 2016) and indicate the connection of DH activity to soil respiration and ULO removal. Consequently, it can be supposed that EOM has a stimulatory effect on both the microbial activity and abundance.

3.2.3. EOM effect on the bacterial community structure and composition during soil remediation

3.2.3.1. 16S amplicon sequencing results and alpha diversity. 16S amplicon sequencing was carried out in order to understand the effect of EOM supplementation on the microbial community of the ULO-polluted soils, in comparison with those that were subjected to conventional bioremediation treatments. Next-generation sequencing analysis of bacterial communities yielded a total of 4132,994 valid reads from the 95 samples. An average of 43,505 sequences per sample was then grouped into phylogenetic OTUs (with numbers ranging from 1137 to 1401) at a clustering threshold of 97% sequence identity. Owing to the possible limits of this method, some of the sequences could not be classified into any known genus and hence were assigned as unclassified. Visualization of the rarefaction curves of the OTUs (Fig. S2), calculated for every treatment at the onset, at the end of the first decay period (20th day), and at the end of the experiment (60th day), revealed that each curve reached the saturation plateau at around 40–50,000 reads. These results indicate that the sequencing depth was reasonable and a higher number of reads would not further contribute to the total number of OTUs (Wu et al., 2017; Hong et al., 2015).

The results of sequence quality and microbial diversity within a community (alpha diversity parameters) under different treatments at days 0, 20, and 60 are shown in Table S2. In all treated soils, species richness and diversity, represented by the number of OTUs, Chao 1, and Faith's PD (Wei et al., 2020), increased significantly during the first 20 days of incubation, possibly due to the optimization of environmental parameters (e.g., soil moisture, NPK treatment, or EOM addition). As the easily biodegradable fraction of the hydrocarbons was likely depleted and/or the bioavailability of toxic compounds might have increased, both richness and diversity gradually declined to the end of the bioremediation experiment (60th day). In contrast, abundance and evenness of species, represented by Shannon and Simpson indices (Wu et al., 2017), diminished constantly over time. These changes were more pronounced in the case of EOM-supplemented soils. BS+EOM and BAS+EOM reached the lowest values of all alpha diversity indices by the end of the experimental period. Nevertheless, the diversity parameters of NA mostly remained higher and changed less than those of any other treatment. In general, microbial communities became more diverse during the first phase of TPH biodegradation, followed by a diversity decrease during the second phase in all of the soils; however, their overall homogeneity constantly decreased throughout the whole bioremediation. Similarly to our results, in aged petroleum-contaminated soils, increased TPH biodegradation alongside increased alpha diversity was observed by other authors (Liu et al., 2020; Wu et al., 2020), while examples of gradually decreasing alpha diversity parameters have also been reported (Pacwa-Płociniczak et al., 2020; Sun et al., 2014).

3.2.3.2. Taxonomic composition and community structure. Fig. S3 presents the microbial community composition at the phylum level based on the ratio of the sequences from the V3–V4 16S rRNA gene region. During the bioremediation experiment, *Proteobacteria* and *Actinobacteriota* were the predominant phyla in all of the soil samples, with relative abundance in the range of 50–76%, collectively. The microbial communities of chronically hydrocarbon-polluted soils are often dominated by *Proteobacteria* and *Actinobacteriota*, and the latter is essentially involved in SOM decomposition or soil nutrient cycling (Pacwa-Płociniczak et al., 2020; Prince et al., 2018; Yang et al., 2014). Both phyla are considered as important hydrocarbon-degraders (Prince et al., 2018; Fuentes et al., 2016). At the beginning of the experiment, *Bacteroidota* accounted for 8–9% of the total reads, which increased to 15–17% in all treated soils after 20 days of incubation, and remained steady until the end of the remediation procedure. This observation can be explained by the decrease in both the TPH level and the metabolic activity of degraders during the second phase of biodegradation, since *Bacteroidota* can be negatively affected by the high initial hydrocarbon concentration or outcompeted by hydrocarbonoclastic bacteria (Kim and Kwon, 2010). Although *Acidobacteriota* is ubiquitous in various soil habitats, constituting an average of 20% of global bacteria (Greening et al., 2015), it had only a low relative abundance (5–6%) in the tested soils, which further decreased during the second phase in the case of each treatment (2–3%), with the only exception of NA (5%), presumably due to the formation of by-products from ULO biodegradation. The majority of the phyla with only a smaller fraction of the total bacteria, such as *Chloroflexi, Myxococcota, Planctomycetota, Patescibacteria, Verrucomicrobiota, Gemmatimonadota, Deinococcota,* and *Firmicutes*, were also observed by previous studies as members of the microbial assemblage in oil-contaminated soils (Liu et al., 2020; Gałązka et al., 2018).

According to their frequencies measured on day 20, KCM-B-112, *Flavobacterium*, *Mycobacterium*, *Lacunisphaera*, *Thermomonas*, *Proteiniphilum*, *Williamsia*, an unclassified *Porticoccaceae* (C1-B045), *Extensimonas*, *Azospira*, *Cavicella*, *Comamonas*, *Ferrovibrio*, and *Geobacter* became predominant in all of the ULO-polluted soil samples with respective percentage ranges of 10–17%, 3–5%, 3–4%, 2–5%, 2–3%, 1–3%, 1–2%, 1–2%, 1–2%, 1–3%, 1–2%, 0.1–1.4%, 0.8–1.4%, and 1–2% (Fig. S4). From these genera, however, only KCM-B-112 (12–15%), *Flavobacterium* (3–11%), *Mycobacterium* (6–9%), *Thermomonas* (3–5%), *Williamsia* (2–3%), C1-B045 (2–3%), and *Geobacter* (0.5–1.3%) remained prevalent until the end of the 60-day-long incubation. Our findings are consistent with the previous studies, which observed these genera in oil-polluted soils. Both KCM-B-112 and *Flavobacterium* inhabit chronically oil-polluted environments (Chaudhary et al., 2019; Chaudhary and Kim, 2018; Chikere et al., 2019; Hershey et al., 2018). *Thermomonas* can be associated with hydrocarbon degradation in weathered soil (Singleton et al., 2013), while the members of *Mycobacterium* and *Williamsia* are known PAH-degraders (Dudhagara and Dave, 2018; Hennessee et al., 2009; Blanco-Enríquez et al., 2018; Bell et al., 2016). C1-B045 is mainly detected in oil-degrading marine microbial communities (Uribe-Flores et al., 2019; Peng et al., 2020); however, it has also been observed in petroleum-contaminated terrestrial habitats (Chikere et al., 2019; Brzeszcz et al., 2020). The increased relative abundance of anaerobic bacterial genera such as *Geobacter* (Lovley et al., 2011) indicates that, despite the mixing of ULO-polluted soils every 2 days, the aeration was insufficient to prevent the formation of oxygen-deficient microhabitats.

The results also showed that, despite the ubiquity of the genus in contaminated environments (Kis et al., 2017), the ULO-polluted composite soil showed a scarcity of *Rhodococcus* (Fig. 1F and Fig. S4). The

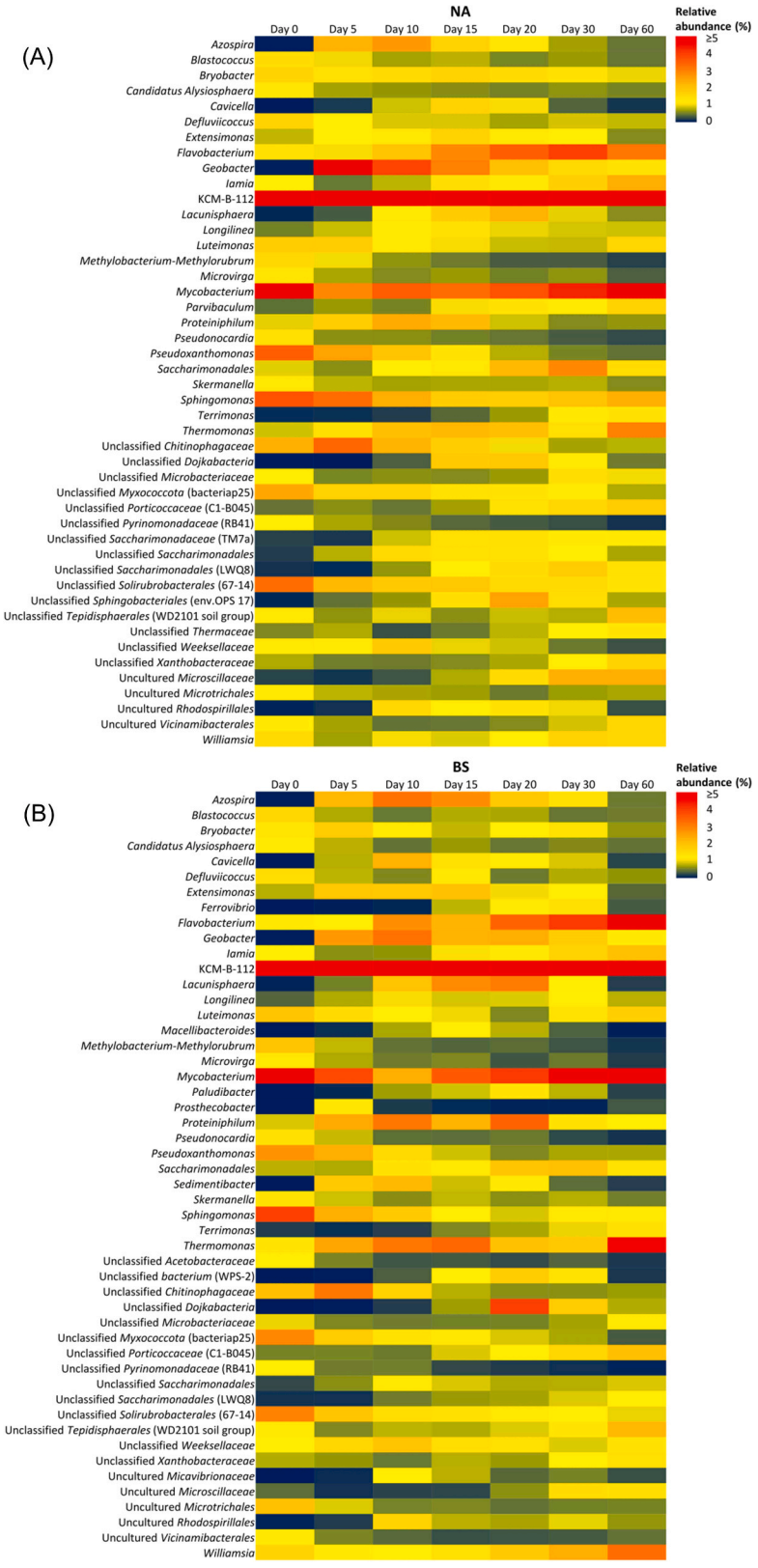

Fig. 3. Heatmap plots, showing the changes of the most abundant bacterial genera in the polluted soils subjected to (A) natural attenuation (NA), (B) biostimulation (BS), (C) biostimulation, and the addition of the extracellular organic matter from *Micrococcus luteus* (BS+EOM); (D) bioaugmentation combined with biostimulation (BAS); and (E) bioaugmentation combined with biostimulation and EOM addition (BAS+EOM), over the experimental period. The heatmaps depict the distribution of the relative abundance for each genus. Every genus was considered to be abundant in the analysis, which reached the minimum of 1% relative abundance on at least one sampling day during the experiment. The degree of color depth indicates the numerical magnitude; a larger percentage value is represented by a redder color.

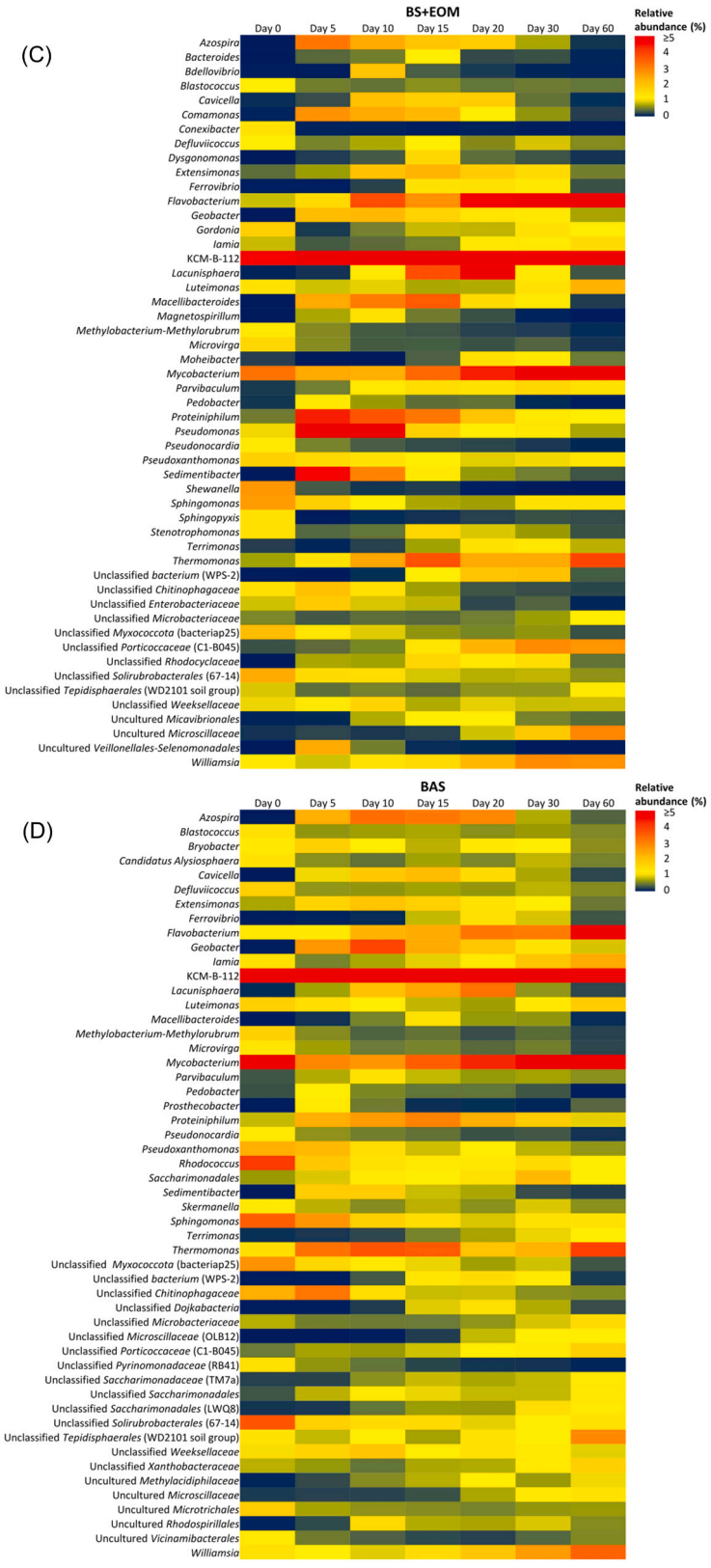

Fig. 3. (*continued*).

inoculation of *Rhodococcus qingshengii* KAG C and *Rhodococcus erythropolis* PR4 increased the relative abundance of *Rhodococcus* to 4–5% in BAS and BAS+EOM; nonetheless, they accounted for nearly 80% of the total cultivable AHB cell counts at the beginning of the experiment. This discrepancy indicated the major presence of VBNC bacteria in our experimental soil, suggesting that the supplementation of Rpf-containing EOM could further impact the composition of the microbial assemblage. During the early phase of biodegradation, the abundance of augmented *Rhodococcus* decreased significantly to 1–2%, and then remained steady throughout the second phase. Although

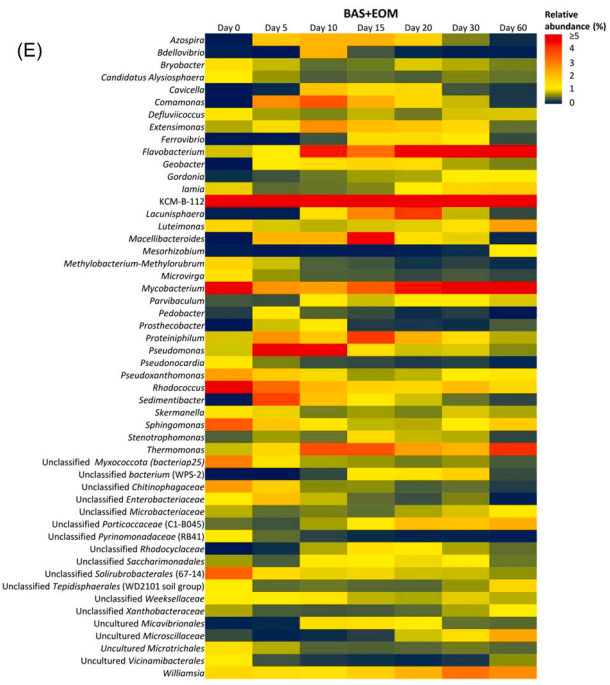

Fig. 3. (*continued*).

previous studies demonstrated that the introduction of the hydrocarbon-degrader *Rhodococcus erythropolis* CD 130 and CD 167 strains to petroleum-contaminated soil caused only temporary changes in the indigenous microbiome and they were undetectable after 42 days (Pacwa-Płociniczak et al., 2019; Pacwa-Płociniczak et al., 2020), we found that *R. qingshengii* KAG C and *R. erythropolis* PR4 were able to survive moderately and integrate into the autochthonous bacterial community of the ULO-polluted soil.

It should be noted that the analysis of the most abundant genera exclusively on the selected sampling days (0, 20, and 60 according to the two biodegradation phases) might mask short- term shifts in the bacterial community, induced by various bioremediation approaches. To avoid these biases from data selection, a more detailed analysis of the dynamic change of microbial communities is shown in Fig. 3. Heatmap plots were created at the genus level, involving only those genera that reached a minimum of 1% relative abundance on at least one sampling day during the experimental period.

In all of the soils, KCM-B-112, belonging to the family *Acidithiobacillaceae*, was the most dominant genus throughout the whole incubation, presumably due to its resistance to elevated heavy metal and hydrocarbon concentrations (Hershey et al., 2018; Marti et al., 2017), which were measured in our experimental soils (Table S1 and Fig. 1A). Combustion products, heavy metals, PCBs, and PAHs are accumulated in used lubricant oils (Pinheiro et al., 2017a), which might provide an explanation for the constantly high relative abundance of *Mycobacterium* (Fig. 3). The members of this genus are often capable of degrading high-molecular-weight hydrocarbons, including even PAHs with four or more benzene rings (Dudhagara and Dave, 2018). Following a slight decrease in their relative abundance, the ratios of the genera *Luteimonas*, *Iamia*, and C1-B045 generally increased during the second phase of biodegradation. This is consistent with previous reports on the late-stage bloom and activity of *Iamia* and C1-B045, which indicated an important yet unknown function of these genera in the aerobic bioremediation processes of environments polluted with aliphatic and polycyclic hydrocarbons (Uribe-Flores et al., 2019; Militon et al., 2010). In contrast, the relative abundances of *Azospira*, *Lacunisphaera*, *Extensimonas*, *Geobacter*, and *Proteiniphilum* showed the opposite changes: the ratios of these genera reached their maximum in the second half of the first biodegradation phase (10–20 days) and then gradually decreased during the second phase. Nitrogen fixation by *Azospira* could serve as an additional nitrogen source in all treated soils (Abed et al., 2014), further promoting the activity of indigenous hydrocarbonoclastic bacteria. However, the decreased abundance of this genus might indicate its sensitivity to the increased bioavailability of toxic ULO compounds or the accumulation of harmful by-products from ULO biodegradation. Although *Lacunisphaera* is not directly associated with hydrocarbon degradation according to the literature, it has been detected in contaminated environments, including trichloroethene-polluted groundwater or alkylbenzene-containing sewage (Wang et al., 2019; Zheng et al., 2020). Thus, its thriving after 15–20 days of bioremediation might be a result of mutualistic metabolic interactions with other bacteria in our experimental soils. *Extensimonas* can inhabit both pristine and polluted man-made environments (Willems, 2014). The generation of the anaerobic hydrocarbon-degrader genera *Geobacter* and *Proteiniphilum* was possibly due to the insufficient aeration of the remediated soils (Lovley et al., 2011; Larsen et al., 2009). In general, *Flavobacterium*, *Thermomonas*, and *Williamsia* had increasing abundances during the soil rehabilitation experiment. Members of *Flavobacterium* occur in oil-affected soils (Chaudhary et al., 2019; Chaudhary and Kim, 2018). In weathered soil, *Thermomonas* can be involved in hydrocarbon biodegradation, but unlike *Williamsia*, it is not associated with PAH removal (Singleton et al., 2013). After the easily biodegradable ULO fractions were possibly depleted, intermediates and by-products from ULO removal were formed, as well as the bioavailability of toxic compounds was increased by biosurfactant-producing bacteria, *Williamsia* could increase in the last stage due to its ability to degrade PAHs or PCBs (Blanco-Enríquez et al., 2018; Bell et al., 2016; Yadav and Yadav, 2019). *Sphingomonas* and *Pseudoxanthomonas* are known for their abilities to degrade various environmental pollutants, including diesel oil, crude oil, aliphatic hydrocarbons (C_7–C_{33}), PAHs, and PCBs (Koshlaf et al., 2020; Kertesz and Kawasaki, 2010; Leys et al., 2004). Nevertheless, both genera dramatically decreased in abundance until the late stage, and they then increased again by the end of the experiment. This trend might indicate that *Sphingomonas* and *Pseudoxanthomonas* were outcompeted by newly stimulated fast-growers in the early phase, and following the depletion of easily available hydrocarbons, they started to recolonize the

soils. Since all of the above-mentioned genera were found in each soil (NA, BS, BAS, BS+EOM, BAS+EOM), it can be hypothesized that their changes were primarily induced by the changes in soil moisture. However, their activity was indeed further enhanced by nutrient stimulation or EOM addition (Fig. 1B, C, G, H).

The genera *Ferrovibrio*, *Sedimentibacter, Macellibacteroides*, and WPS-2 were detected at over 1% relative abundance only in NPK-fertilized soils, including BS, BAS, BS+EOM, and BAS+EOM. Their increased ratios reached a maximum in the second half of the first biodegradation phase (10–20 days) and then they decrease in abundance (Fig. 3B, C, D, E). While WPS-2, owing to its putative ecological role in autotrophic CO_2 fixation, typically prefers oxygen-rich environments (Sheremet et al., 2020; Ward et al., 2019), the members of *Ferrovibrio*, *Sedimentibacter*, and *Macellibacteroides* are facultative or strict anaerobic bacteria (Lechner, 2015; Jabari et al., 2012; Baldani et al., 2014), corroborating the formation of oxygen-deficient microhabitats despite the soil mixing every 2 days. Each of them is found in polluted environments. WPS-2 was first discovered in PCB-contaminated soil (Ward et al., 2019). *Sedimentibacter*, *Macellibacteroides*, and *Ferrovibrio* are present in hydrocarbon-degrading communities (Berdugo-Clavijo et al., 2012; Brzeszcz et al., 2020; Cai et al., 2020b; Tischer et al., 2013), indicating their possible roles in environmental decontamination.

In response to EOM supplementation, *Pseudomonas* became the most dominant bacterial genus (13–15%) in BS+EOM and BAS+EOM after 5 days (Fig. 3C and E), after which its abundance dramatically decreased by the end of the first biodegradation phase. The changes in the relative abundance of *Comamonas* showed similar trends in EOM-treated soils. Both genera are known for their ability to degrade hydrocarbons (Prince et al., 2018; Goyal and Zylstra, 1996; Xu et al., 2018; De La Cueva et al., 2016), indicating their potential role in the enhanced ULO biodegradation observed in BS+EOM and BAS+EOM during the early phase (Fig. 2A). The hydrocarbonoclastic genus *Gordonia* increased discernibly throughout the experimental period (Silva et al., 2019), while the ratio of *Stenotrophomonas* reached an early-phase maximum (Fig. 3C and E). The members of *Stenotrophomonas* can be resistant to heavy metals and also able to decompose a wide range of xenobiotics, including PAHs or pyrene (Prince et al., 2018; Ryan et al., 2009; Arulazhagan et al., 2017). We supposed that the resuscitation of these genera by the supplementation of Rpf-containing EOM greatly contributed to the enhanced ULO removal in BS+EOM and BAS+EOM. Our findings are consistent with the research of Su and colleagues, who reported the predominance of *Pseudomonas* and *Stenotrophomonas* in an Rpf-responsive bacterial community of PCB-contaminated soil (Su et al., 2021). The increase of unclassified bacterial genera belonging to the *Enterobacteriaceae* and *Rhodocyclaceae* families indicates the EOM-promoted presence of additional potential oil-degraders. Therefore, our results further corroborate that the Rpf content of EOM has a resuscitative or stimulatory effect on both Gram-positive and -negative bacteria, as described in earlier studies (Su et al., 2021; Su et al., 2013; Oliver, 2010). Although a high heavy metal concentration might retard their activities, the generation of predatory bacteria such as *Bdellovibrio* and an uncultured genus, belonging to the order *Micavibrionales*, was possibly promoted by the increased CFUs in BS+EOM and BAS+EOM (Fig. 1D and E) due to EOM addition (Varon and Shilo, 1981; Farhan Ul Haque et al., 2019). Most of the above-mentioned EOM-responsive taxa are generally found in environmental samples; however, some of their members can occasionally cause human disease (Bennett et al., 2014). Consequently, the safe environmental applicability of EOM requires further investigation and its future integration into practical bioremediation should proceed carefully.

A Venn diagram was generated to demonstrate the common and unique genera among all of the treatments (Fig. S5). However, for the sake of simplicity, only those genera that reached the minimum of 1% relative abundance on at least one sampling day during the experiment were again involved in the analysis. A total of 75 genera were found to fit this criterion, of which 36% were then common to all treatments. The total numbers of genera were 46, 50, 51, 52, and 52 in NA, BS, BS+EOM, BAS, and BAS+EOM, respectively, and the numbers of unique genera in the respective treatments were 2, 3, 8, 2, and 1. Thus, the ratios of these unique genera in the five bioremediation treatments were 4.3%, 6%, 15.7%, 3.8%, and 1.9%, respectively. Overall, 17 of the total of 75 genera (22.7%) belonged exclusively to EOM-supplemented samples, of which 8 genera (10.6%) were found in both BS+EOM and BAS+EOM, indicating a stimulatory or resuscitative effect of EOM on potentially functional hydrocarbonoclastic and PAH-degrading bacteria such as the members of *Pseudomonas*, *Gordonia*, *Comamonas*, or *Stenotrophomonas* (Prince et al., 2018; Xu et al., 2018). These results are in line with the latest studies that revealed Rpf-responsive populations with potential functions of environmental remediation in the phyla *Proteobacteria* and *Actinobacteria* (Su et al., 2019a; Su et al., 2019b; Yu et al., 2020).

PCoA was performed to visualize the diversity among microbial communities (beta diversity) of the ULO-contaminated soils, subjected to various soil remediation methods (Fig. 4). The PCoA analyses showed that, despite the introduction of exogenous *Rhodococcus* strains into the soils (bioaugmentation), the microbial community compositions of NA, BS, BS+EOM, BAS, and BAS+EOM did not differ from each other at the onset, but started to diverge during the experimental period. Interestingly, the community structure of any sample taken at various incubation times was more separated from each other than the groups of individual treatments within the same sampling day. After 20 days of incubation, the microbial communities of BS and BAS tended to be clustered together. BS+EOM and BAS+EOM also seemed to have similar microbiomes. However, both BS and BAS were closer to NA than to their EOM-supplemented counterparts. At the end of the bioremediation experiment (60 days), all of the treatments slightly gathered together, indicating decreased differences in the biodiversity of their microbial communities. Pacwa-Płociniczak and colleagues (Pacwa-Płociniczak et al., 2020) also observed a drop in the variance of the composition of microbial communities in bioaugmented aged petroleum-contaminated soils throughout the experimental period.

3.2.4. Soil phytotoxicity

As a decrease in TPH contamination is not always associated with reduced soil toxicity, it is indispensable to assess information about the soil condition after any remediation treatment (Jiang et al., 2016). To this end, the germination index (GI%) of Indian mustard (*Brassica juncea*) was used to evaluate initial (t_0) soil quality and the ecotoxicological effects of the ULO removal triggered by conventional and EOM-supplemented bioremediation approaches (t_{60}). Results were normalized using the germination and root length data obtained in the uncontaminated control soil, which revealed that ULO-pollution alone resulted in a reduced GI (43%) of the initial composite soil (t_0). The ecotoxicity assessment showed that the germination indices of NA, BS, BS+EOM BAS, and BAS+EOM after 60 days with the values of 36%, 24%, 13%, 25%, and 24%, respectively, were significantly lower than that for the initial soil condition (Fig. 5). These changes followed similar trends to the decrease of final TPH concentrations; therefore, it can be assumed that the reduction in GI% of mustard seeds in each treated soil was due to the accumulation of toxic by-products of ULO removal or even to the increased bioavailability of hazardous ULO compounds induced by the surfactant production of certain bacteria. Although previous studies are rather controversial regarding the positive (Poi et al., 2017; Nwankwegu et al., 2016; Graj et al., 2013) or adverse effects (Jiang et al., 2016; Dorn and Salanitro, 2000) of TPH decontamination on plant germination, our results are in line with other reports, suggesting that phytotoxic effects can be triggered by both the nature (structure, molecular weight, etc.) and the concentration of the hydrocarbon present (Khan et al., 2018; Ogbo, 2009).

To further understand the effect of conventional and EOM-supplemented rehabilitation techniques on ULO-contaminated soils, vitality and membrane integrity of the mustard seedlings' root apical meristem were also investigated (Fig. S6). These two parameters refer to

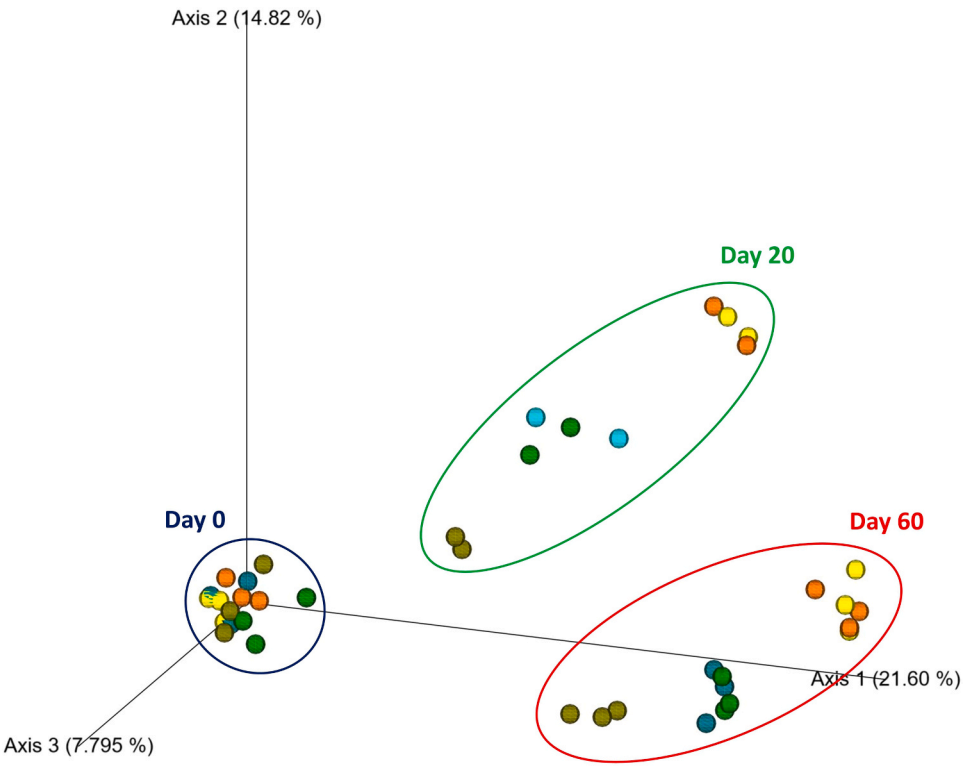

Fig. 4. Principal coordinate analyses (PCoA) plot based on the Bray–Curtis similarities of the OTU-based bacterial community analysis in the polluted soils subjected to natural attenuation (NA, khaki spheres), biostimulation (BS, green spheres), biostimulation, and the addition of the extracellular organic matter from *Micrococcus luteus* (BS+EOM, yellow spheres); bioaugmentation combined with biostimulation (BAS, blue spheres); and bioaugmentation combined with biostimulation and EOM addition (BAS+EOM, orange spheres) on day 0, day 20, and day 60.

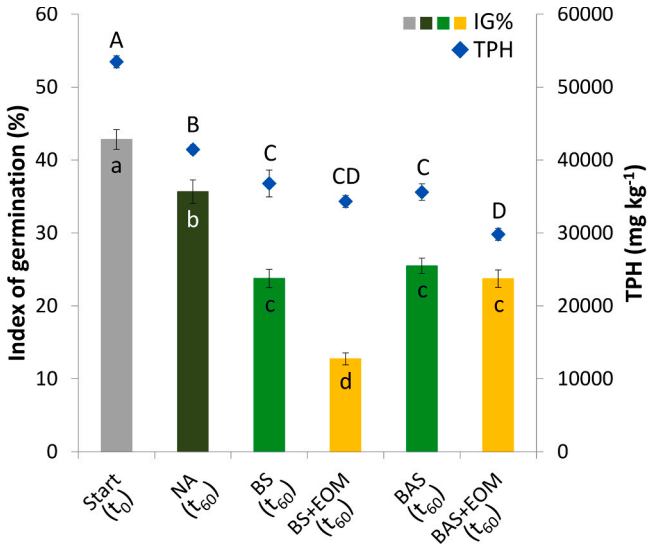

Fig. 5. (A) Germination index of mustard seedlings (colored bars) and (B) concentration of total petrol hydrocarbons (TPH, blue diamonds) at the onset (t_0) and after 60 days (t_{60}) for each treated soil. Different letters in the same data set represent a statistically significant difference at $p \leq 0.05$ ($n \geq 6$).

the overall viability of the root apical meristem, which is a sensitive stress indicator in the early phase of plant development (Feigl et al., 2019). Fluorescent staining revealed that, in comparison with the values measured in the initial ULO-contaminated composite soil (t_0), the vitality of the meristematic zone increased (according to the increase of FDA fluorescence), while the amount of dead cells decreased significantly (according to the decrease of PI fluorescence) after soil remediation (t_{60}). Consequently, in all treated soils, increased overall viability of the mustard seedlings' apical root meristem was observed.

Soil phytotoxicity demonstrated that, although the germination rate of Indian mustard was inhibited presumably due to the accumulation of intermediates and by-products from ULO biodegradation, the germinated seedlings became more viable and vital when grown in the remediated soils. Most studies rely exclusively on germination indices to evaluate soil phytotoxicity after soil bioremediation treatments. In this study, however, vitality and membrane integrity of the mustard seedlings' root apical meristem were included in the soil phytotoxicity measurements in order to obtain a broader view of the effectiveness of remediation. Although this study did not aim at revealing the reasons behind the experienced changes in the responses of the root apical meristems, our seemingly contradictory results imply that ecotoxicological responses induced in plants are much more complicated than being characterized by simply the inhibition of germination or root development. Our findings further corroborate that a reduction in TPH and decreased soil toxicity do not necessarily have a direct correlation; thus, monitoring the hydrocarbon concentration alone is insufficient for assessing environmental risk following soil remediation (Khan et al., 2018; Jiang et al., 2016).

4. Conclusions

The novel application of Rpf-containing EOM from *Micrococcus luteus* increased the decontamination efficacy of aged ULO-polluted soils by enhancing the microbial activity and culturable cell counts, and promoting the proliferation of unique EOM-responsive hydrocarbonoclastic bacterial genera such as *Pseudomonas*, *Comamonas*, *Stenotrophomonas*, and *Gordonia*. EOM also enhanced the ULO biodegradation performance of a bacterial inoculum, comprising previously not resuscitated nor EOM-treated strains (*Rhodococcus qingshengii* KAG C and *R. erytropolis* PR4). Soil phytotoxicity assessments revealed that a reduction in TPH and decreased soil toxicity did not necessarily have a direct correlation. The accelerated ULO removal promoted by EOM supplementation substantiate that, compared with physicochemical and conventional bioremediation approaches, EOM-stimulation of the autochthonous microbiota can be justified both environmentally and economically to decontaminate long term ULO-contaminated soils. Nevertheless, when

an urgent remediation is needed, EOM-enhanced bioaugmentation might significantly increase the efficiency of the rehabilitation processes of freshly hydrocarbon-contaminated environments. Overall, the findings of this study provide a deep insight into the potential applicability of EOM and its effects on both the soil microbial activity and community structure. However, since some members of the EOM-responsive genera can occasionally cause human disease, the safe environmental application of EOM requires further investigations and its future integration into practical bioremediation should be carried out carefully.

Funding

This research was supported by the European Union and the Hungarian State in the framework of the EFOP-3.6.2-16-2017-00010.

CRediT authorship contribution statement

A.B., G.R. and K.P.: Conceptualization. **A.B., G.F. and K.L.:** Data curation. **A.B., G.F. and K.L.:** Formal analysis. **G.R.:** Funding acquisition. **A.B., N.B., G.F. and Á.S.:** Investigation. **A.B., N.B., G.F. and Á. D.:** Methodology. **A.B., G.R. and K.P.:** Project administration. **G.F., G. R. and K.P.:** Resources. **G.F., K.L., G.R.:** Software. **G.R. and K.P.:** Supervision. **A.B., N.B., G.F. and Á.D.:** Validation. **A.B.:** Visualization. **A.B.:** Writing - original draft. **A.B., G.F., K.L., G.R. and K.P.:** Writing - review & editing.

Declaration of Competing Interest

The authors declare that they have no known competing financial interests or personal relationships that could have appeared to influence the work reported in this paper.

Acknowledgments

The authors thank Hungarian State Railways for making their work possible. The support and advice of Péter Tóth (MÁV Szolgáltató Központ Zrt., Hungary), Bernadett Kolozsi (MÁV Szolgáltató Központ Zrt., Hungary), and Gyula Gyarmati (MÁV-START Zrt., Hungary) are gratefully acknowledged. *Brassica* seeds were kindly provided by Réka Szőllősi (Department of Plant Biology, University of Szeged, Hungary). The authors would also like to thank Izabella Babcsányi (Department of Physical Geography and Geoinformatics, University of Szeged, Hungary) for the quantification of heavy metals. Finally, the authors would like to express their gratitude toward Ms. Sarolta Papp for the excellent technical assistance.

Appendix A. Supporting information

Supplementary data associated with this article can be found in the online version at doi:10.1016/j.jhazmat.2021.125996.

References

Abed, R.M.M., Al-Kharusi, S., Prigent, S., Headley, T., 2014. Diversity, distribution and hydrocarbon biodegradation capabilities of microbial communities in oil-contaminated cyanobacterial mats from a constructed wetland. PLoS One 9, 114570. https://doi.org/10.1371/journal.pone.0114570.

Agarry, S.E., Aremu, M.O., Aworanti, O.A., 2013. Kinetic modelling and half-life study on bioremediation of soil co-contaminated with lubricating motor oil and lead using different bioremediation strategies. Soil Sediment Contam. Int. J. 22, 800–816. https://doi.org/10.1080/15320383.2013.768204.

Arulazhagan, P., Al-Shekri, K., Huda, Q., Godon, J.J., Basahi, J.M., Jeyakumar, D., 2017. Biodegradation of polycyclic aromatic hydrocarbons by an acidophilic Stenotrophomonas maltophilia strain AJH1 isolated from a mineral mining site in Saudi Arabia. Extremophiles 21, 163–174. https://doi.org/10.1007/s00792-016-0892-0.

Baldani, J., Videira, S., dos Santos Teixeira, K., Reis, V., de Oliveira, A., Schwab, S., de Souza, E., Pedraza, R., Baldani, V., Hartmann, A., 2014. The family Rhodospirillaceae. In: Rosenberg, E., Delong, E., Lory, S., Stackebrandt, E., Thompson, F. (Eds.), The Prokaryotes-Alphaproteobacteria and Betaproteobacteria. Springer-Verlag, New York, pp. 533–618.

Barwick, V.J., Ellison, S.L.R., Rafferty, M.J.Q., Farrant, T.J., 1998. Evaluation of carbon disulfide as an alternative to carbon tetrachloride for the determination of hydrocarbon oils in water by infra-red spectrophotometry. Int. J. Environ. Anal. Chem. 72, 235–246. https://doi.org/10.1080/03067319808035895.

Bekins, B.A., Brennan, J.C., Tillitt, D.E., Cozzarelli, I.M., Illig, J.M.G., Martinović-Weigelt, D., 2020. Biological effects of hydrocarbon degradation intermediates: is the total petroleum hydrocarbon analytical method adequate for risk assessment? Environ. Sci. Technol. 54, 11396–11404. https://doi.org/10.1021/acs.est.0c02220.

Bell, T.H., Stefani, F.O.P., Abram, K., Champagne, J., Yergeau, E., Hijri, M., St-Arnaud, M., 2016. A diverse soil microbiome degrades more crude oil than specialized bacterial assemblages obtained in culture. Appl. Environ. Microbiol. 82, 5530–5541. https://doi.org/10.1128/AEM.01327-16.

Bennett, J.E., Dolin, R., Blaser, M.J., 2014. Mandell, Douglas, and Bennett's Principles and Practice of Infectious Diseases. Elsevier Inc,. https://doi.org/10.1016/s1473-3099(10)70089-x.

Berdugo-Clavijo, C., Dong, X., Soh, J., Sensen, C.W., Gieg, L.M., 2012. Methanogenic biodegradation of two-ringed polycyclic aromatic hydrocarbons. FEMS Microbiol. Ecol. 81, 124–133. https://doi.org/10.1111/j.1574-6941.2012.01328.x.

Blanco-Enríquez, E., Zavala-Díaz de la Serna, F., Peralta-Pérez, M., Ballinas-Casarrubias, L., Salmerón, I., Rubio-Arias, H., Rocha-Gutiérrez, B., 2018. Characterization of a microbial consortium for the bioremoval of Polycyclic Aromatic Hydrocarbons (PAHs) in water. IJERPH 15, 975. https://doi.org/10.3390/ijerph15050975.

Bodor, A., Bounedjoum, N., Vincze, G.E., Erdeiné Kis, Á., Laczi, K., Bende, G., Szilágyi, Á., Kovács, T., Perei, K., Rákhely, G., 2020a. Challenges of unculturable bacteria: environmental perspectives. Rev. Environ. Sci. Biotechnol. 19, 1–22. https://doi.org/10.1007/s11157-020-09522-4.

Bodor, A., Petrovszki, P., Erdeiné Kis, Á., Vincze, G.E., Laczi, K., Bounedjoum, N., Szilágyi, Á., Szalontai, B., Feigl, G., Kovács, K.L., Rákhely, G., Perei, K., 2020b. Intensification of ex situ bioremediation of soils polluted with used lubricant oils: a comparison of biostimulation and bioaugmentation with a special focus on the type and size of the inoculum. IJERPH 17, 4106. https://doi.org/10.3390/ijerph17114106.

Bolyen, E., Rideout, J.R., Dillon, M.R., Bokulich, N.A., Abnet, C.C., Al-Ghalith, G.A., Alexander, H., Alm, E.J., Arumugam, M., Asnicar, F., Bai, Y., Bisanz, J.E., Bittinger, K., Brejnrod, A., Brislawn, C.J., Brown, C.T., Callahan, B.J., Caraballo-Rodríguez, A.M., Chase, J., Cope, E.K., Da Silva, R., Diener, C., Dorrestein, P.C., Douglas, G.M., Durall, D.M., Duvallet, C., Edwardson, C.F., Ernst, M., Estaki, M., Fouquier, J., Gauglitz, J.M., Gibbons, S.M., Gibson, D.L., Gonzalez, A., Gorlick, K., Guo, J., Hillmann, B., Holmes, S., Holste, H., Huttenhower, C., Huttley, G.A., Janssen, S., Jarmusch, A.K., Jiang, L., Kaehler, B.D., Bin Kang, K., Keefe, C.R., Keim, P., Kelley, S.T., Knights, D., Koester, I., Kosciolek, T., Kreps, J., Langille, M.G. I., Lee, J., Ley, R., Liu, Y.X., Loftfield, E., Lozupone, C., Maher, M., Marotz, C., Martin, B.D., McDonald, D., McIver, L.J., Melnik, A.V., Metcalf, J.L., Morgan, S.C., Morton, J.T., Naimey, A.T., Navas-Molina, J.A., Nothias, L.F., Orchanian, S.B., Pearson, T., Peoples, S.L., Petras, D., Preuss, M.L., Pruesse, E., Rasmussen, L.B., Rivers, A., Robeson, M.S., Rosenthal, P., Segata, N., Shaffer, M., Shiffer, A., Sinha, R., Song, S.J., Spear, J.R., Swafford, A.D., Thompson, L.R., Torres, P.J., Trinh, P., Tripathi, A., Turnbaugh, P.J., Ul-Hasan, S., van der Hooft, J.J.J., Vargas, F., Vázquez-Baeza, Y., Vogtmann, E., von Hippel, M., Walters, W., Wan, Y., Wang, M., Warren, J., Weber, K.C., Williamson, C.H.D., Willis, A.D., Xu, Z.Z., Zaneveld, J.R., Zhang, Y., Zhu, Q., Knight, R., Caporaso, J.G., 2019. Reproducible, interactive, scalable and extensible microbiome data science using QIIME 2. Nat. Biotechnol. 37, 852–857. https://doi.org/10.1038/s41587-019-0209-9.

Botas, J.A., Moreno, J., Espada, J.J., Serrano, D.P., Dufour, J., 2017. Recycling of used lubricating oil: evaluation of environmental and energy performance by LCA. Resour. Conserv. Recycl. 125, 315–323. https://doi.org/10.1016/j.resconrec.2017.07.010.

Bounedjoum, N., Bodor, A., Laczi, K., Kis, Á.E., Rákhely, G., Perei, K., 2018. Assessment of potentially functional hydrocarbon-degrader bacterial communities in response to Micrococcus luteus EOM using culture-dependent and culture-independent methods. New Biotechnol. 44, S134–S135. https://doi.org/10.1016/j.nbt.2018.05.1091.

Brzeszcz, J., Kapusta, P., Steliga, T., Turkiewicz, A., 2020. Hydrocarbon removal by two differently developed microbial inoculants and comparing their actions with biostimulation treatment. Molecules 25, 661. https://doi.org/10.3390/molecules25030661.

Cai, J., Liu, J., Pan, A., Liu, J., Wang, Y., Liu, J., Sun, F., Lin, H., Chen, J., Su, X., 2020a. Effective decolorization of anthraquinone dye reactive blue 19 using immobilized Bacillus sp. JF4 isolated by resuscitation-promoting factor strategy. Water Sci. Technol. 81, 1159–1169. https://doi.org/10.2166/wst.2020.201.

Cai, X., Yuan, Y., Yu, L., Zhang, B., Li, J., Liu, T., Yu, Z., Zhou, S., 2020b. Biochar enhances bioelectrochemical remediation of pentachlorophenol-contaminated soils via long-distance electron transfer. J. Hazard. Mater. 391, 122213 https://doi.org/10.1016/j.jhazmat.2020.122213.

Chaudhary, D.K., Kim, J., 2018. Flavobacterium naphthae sp. nov., isolated from oil-contaminated soil. Int. J. Syst. Evol. Microbiol 68, 305–309. https://doi.org/10.1099/ijsem.0.002504.

Chaudhary, D.K., Kim, D.U., Kim, D., Kim, J., 2019. Flavobacterium petrolei sp. nov., a novel psychrophilic, diesel-degrading bacterium isolated from oil-contaminated Arctic soil. Sci. Rep. 9, 1–9. https://doi.org/10.1038/s41598-019-40667-7.

Chikere, C.B., Mordi, I.J., Chikere, B.O., Selvarajan, R., Ashafa, T.O., Obieze, C.C., 2019. Comparative metagenomics and functional profiling of crude oil-polluted soils in Bodo West Community, Ogoni, with other sites of varying pollution history. Ann. Microbiol. 69, 495–513. https://doi.org/10.1007/s13213-019-1438-3.

De La Cueva, S.C., Rodríguez, C.H., Cruz, N.O.S., Contreras, J.A.R., Miranda, J.L., 2016. Changes in bacterial populations during bioremediation of soil contaminated with petroleum hydrocarbons. Water Air Soil Pollut. 227, 1–12. https://doi.org/10.1007/s11270-016-2789-z.

Dong, K., Pan, H., Yang, D., Rao, L., Zhao, L., Wang, Y., Liao, X., 2020. Induction, detection, formation, and resuscitation of viable but non-culturable state microorganisms. Compr. Rev. Food Sci. Food Saf. 19, 149–183. https://doi.org/10.1111/1541-4337.12513.

Dorn, P.B., Salanitro, J.P., 2000. Temporal ecological assessment of oil contaminated soils before and after bioremediation. Chemosphere 40, 419–426. https://doi.org/10.1016/S0045-6535(99)00304-5.

Dudhagara, D.R., Dave, B.P., 2018. Mycobacterium as Polycyclic Aromatic Hydrocarbons (PAHs) degrader. In: Mycobacterium – Res. Dev. InTech. https://doi.org/10.5772/intechopen.73546.

Farhan Ul Haque, M., Crombie, A.T., Murrell, J.C., 2019. Novel facultative Methylocella strains are active methane consumers at terrestrial natural gas seeps. Microbiome 7, 1–17. https://doi.org/10.1186/s40168-019-0741-3.

Farsang, A., Babcsányi, I., Ladányi, Z., Perei, K., Bodor, A., Csányi, K.T., Barta, K., 2020. Evaluating the effects of sewage sludge compost applications on the microbial activity, the nutrient and heavy metal content of a Chernozem soil in a field survey. Arab. J. Geosci. 13, 982. https://doi.org/10.1007/s12517-020-06005-2.

Feigl, G., Kolbert, Z., Lehotai, N., Molnár, Á., Ördög, A., Bordé, Á., Laskay, G., Erdei, L., 2016. Different zinc sensitivity of Brassica organs is accompanied by distinct responses in protein nitration level and pattern. Ecotoxicol. Environ. Saf. 125, 141–152. https://doi.org/10.1016/j.ecoenv.2015.12.006.

Feigl, G., Molnár, Á., Szőllősi, R., Ördög, A., Törőcsik, K., Oláh, D., Bodor, A., Perei, K., Kolbert, Z., 2019. Zinc-induced root architectural changes of rhizotron-grown B. napus correlate with a differential nitro-oxidative response. Nitric Oxide – Biol. Chem. 90, 55–65. https://doi.org/10.1016/j.niox.2019.06.003.

Fuentes, S., Barra, B., Gregory Caporaso, J., Seeger, M., 2016. From rare to dominant: a fine-tuned soil bacterial bloom during petroleum hydrocarbon bioremediation. Appl. Environ. Microbiol. 82, 888–896. https://doi.org/10.1128/AEM.02625-15.

Gałązka, A., Grządziel, J., Gałązka, R., Ukalska-Jaruga, A., Strzelecka, J., Smreczak, B., 2018. Genetic and functional diversity of bacterial microbiome in soils with long term impacts of petroleum hydrocarbons. Front. Microbiol. 9, 1923. https://doi.org/10.3389/fmicb.2018.01923.

Goyal, A.K., Zylstra, G.J., 1996. Molecular cloning of novel genes for polycyclic aromatic hydrocarbon degradation from Comamonas testosteroni GZ39. Appl. Environ. Microbiol 62, 230–236. https://doi.org/10.1128/aem.62.1.230-236.1996.

Grace Liu, P.-W., Chang, T.C., Whang, L.-M., Kao, C.-H., Pan, P.-T., Cheng, S.-S., 2011. Bioremediation of petroleum hydrocarbon contaminated soil: effects of strategies and microbial community shift. Int. Biodeterior. Biodegrad. 65, 1119–1127. https://doi.org/10.1016/J.IBIOD.2011.09.002.

Graj, W., Lisiecki, P., Szulc, A., Chrzanowski, Ł., Wojtera-Kwiczor, J., 2013. Bioaugmentation with petroleum-degrading consortia has a selective growth-promoting impact on crop plants germinated in diesel oil-contaminated soil. Water Air Soil Pollut. 224, 1–15. https://doi.org/10.1007/s11270-013-1676-0.

Greening, C., Carere, C.R., Rushton-Green, R., Harold, L.K., Hards, K., Taylor, M.C., Morales, S.E., Stott, M.B., Cook, G.M., 2015. Persistence of the dominant soil phylum Acidobacteria by trace gas scavenging. Proc. Natl. Acad. Sci. USA 112, 10497–10502. https://doi.org/10.1073/pnas.1508385112.

Heiri, O., Lotter, A.F., Lemcke, G., 2001. Loss on ignition as a method for estimating organic and carbonate content in sediments: reproducibility and comparability of results. J. Paleolimnol. 25, 101–110. https://doi.org/10.1023/A:1008119611481.

Hennessee, C.T., Seo, J.S., Alvarez, A.M., Li, Q.X., 2009. Polycyclic aromatic hydrocarbon-degrading species isolated from Hawaiian soils: mycobacterium crocinum sp. nov., Mycobacterium pallens sp. nov., mycobacterium rutilum sp. nov., Mycobacterium rufum sp. nov. and Mycobacterium aromaticivorans sp. nov. Int. J. Syst. Evol. Microbiol. 59, 378–387. https://doi.org/10.1099/ijs.0.65827-0.

Hershey, O.S., Kallmeyer, J., Wallace, A., Barton, M.D., Barton, H.A., 2018. High microbial diversity despite extremely low biomass in a deep karst aquifer. Front. Microbiol. 9, 2823. https://doi.org/10.3389/fmicb.2018.02823.

Hong, C., Si, Y., Xing, Y., Li, Y., 2015. Illumina MiSeq sequencing investigation on the contrasting soil bacterial community structures in different iron mining areas. Environ. Sci. Pollut. Res. 22, 10788–10799. https://doi.org/10.1007/s11356-015-4186-3.

Jabari, L., Gannoun, H., Cayol, J.L., Hedi, A., Sakamoto, M., Falsen, E., Ohkuma, M., Hamdi, M., Fauque, G., Ollivier, B., Fardeau, M.L., 2012. Macellibacteroides fermentans gen. nov., sp. nov., a member of the family Porphyromonadaceae isolated from an upflow anaerobic filter treating abattoir wastewaters. Int. J. Syst. Evol. Microbiol. 62, 2522–2527. https://doi.org/10.1099/ijs.0.032508-0.

Jiang, Y., Brassington, K.J., Prpich, G., Paton, G.I., Semple, K.T., Pollard, S.J.T., Coulon, F., 2016. Insights into the biodegradation of weathered hydrocarbons in contaminated soils by bioaugmentation and nutrient stimulation. Chemosphere 161, 300–307. https://doi.org/10.1016/J.CHEMOSPHERE.2016.07.032.

Kakuk, B., Kovács, K.L., Szuhaj, M., Rákhely, G., Bagi, Z., 2017. Adaptation of continuous biogas reactors operating under wet fermentation conditions to dry conditions with corn stover as substrate. Anaerobe 46, 78–85. https://doi.org/10.1016/J.ANAEROBE.2017.05.015.

Kertesz, M.A., Kawasaki, A., 2010. Hydrocarbon-degrading sphingomonads: sphingomonas, sphingobium, novosphingobium, and sphingopyxis. In: Handb. Hydrocarb. Lipid Microbiol. Springer, Berlin Heidelberg, pp. 1693–1705. https://doi.org/10.1007/978-3-540-77587-4_119.

Khan, M.A.I., Biswas, B., Smith, E., Naidu, R., Megharaj, M., 2018. Toxicity assessment of fresh and weathered petroleum hydrocarbons in contaminated soil- a review. Chemosphere 212, 755–767. https://doi.org/10.1016/j.chemosphere.2018.08.094.

Kim, S.-J., Kwon, K.K., 2010. Bacteroidetes. In: Handb. Hydrocarb. Lipid Microbiol. Springer, Berlin Heidelberg, pp. 1813–1817. https://doi.org/10.1007/978-3-540-77587-4_132.

Kis, Á.E., Laczi, K., Zsíros, S., Kós, P., Tengölics, R., Bounedjoum, N., Kovács, T., Rákhely, G., Perei, K., 2017. Characterization of the Rhodococcus sp. MK1 strain and its pilot application for bioremediation of diesel oil-contaminated soil. Acta Microbiol. Immunol. Hung. 64, 463–482. https://doi.org/10.1556/030.64.2017.037.

Kis, Á., Laczi, K., Zsíros, S., Rákhely, G., Perei, K., 2015. Biodegradation of animal fats and vegetable oils by Rhodococcus erythropolis PR4. Int. Biodeterior. Biodegrad. 105, 114–119. https://doi.org/10.1016/j.ibiod.2015.08.015.

Komukai-Nakamura, S., Sugiura, K., Yamauchi-Inomata, Y., Toki, H., Venkateswaran, K., Yamamoto, S., Tanaka, H., Harayama, S., 1996. Construction of bacterial consortia that degrade Arabian light crude oil. J. Ferment. Bioeng. 82, 570–574. https://doi.org/10.1016/S0922-338X(97)81254-8.

Koshlaf, E., Ball, A.S., 2017. Soil bioremediation approaches for petroleum hydrocarbon polluted environments. AIMS Microbiol. 3, 25–49. https://doi.org/10.3934/microbiol.2017.1.25.

Koshlaf, E., Shahsavari, E., Haleyur, N., Osborn, A.M., Ball, A.S., 2020. Impact of necrophytoremediation on petroleum hydrocarbon degradation, ecotoxicity and soil bacterial community composition in diesel-contaminated soil. Environ. Sci. Pollut. Res. 27, 31171–31183. https://doi.org/10.1007/s11356-020-09339-2.

Laczi, K., Kis, Á., Horváth, B., Maróti, G., Hegedüs, B., Perei, K., Rákhely, G., 2015. Metabolic responses of Rhodococcus erythropolis PR4 grown on diesel oil and various hydrocarbons. Appl. Microbiol. Biotechnol. 99, 9745–9759. https://doi.org/10.1007/s00253-015-6936-z.

Larsen, S.B., Karakashev, D., Angelidaki, I., Schmidt, J.E., 2009. Ex-situ bioremediation of polycyclic aromatic hydrocarbons in sewage sludge. J. Hazard. Mater. 164, 1568–1572. https://doi.org/10.1016/j.jhazmat.2008.08.067.

Lechner, U., 2015. Sedimentibacter. In: Bergey's Man. Syst. Archaea Bact. Wiley, pp. 1–7. https://doi.org/10.1002/9781118960608.gbm00718.

Lee, S.H., Ji, W., Kang, D.M., Kim, M.S., 2018. Effect of soil water content on heavy mineral oil biodegradation in soil. J. Soils Sediments 18, 983–991. https://doi.org/10.1007/s11368-017-1849-3.

Lee, S.-H., Lee, S., Kim, D.-Y., Kim, J., 2007. Degradation characteristics of waste lubricants under different nutrient conditions. J. Hazard. Mater. 143, 65–72. https://doi.org/10.1016/J.JHAZMAT.2006.08.059.

Leys, N.M.E.J., Ryngaert, A., Bastiaens, L., Verstraete, W., Top, E.M., Springael, D., 2004. Occurrence and phylogenetic diversity of sphingomonas strains in soils contaminated with polycyclic aromatic hydrocarbons. Appl. Environ. Microbiol. 70, 1944–1955. https://doi.org/10.1128/AEM.70.4.1944-1955.2004.

Liu, H., Gao, H., Wu, M., Ma, C., Wu, J., Ye, X., 2020. Distribution characteristics of bacterial communities and hydrocarbon degradation dynamics during the remediation of petroleum-contaminated soil by enhancing moisture content. Microbiol. Ecol. 80, 202–211. https://doi.org/10.1007/s00248-019-01476-7.

Lovley, D.R., Ueki, T., Zhang, T., Malvankar, N.S., Shrestha, P.M., Flanagan, K.A., Aklujkar, M., Butler, J.E., Giloteaux, L., Rotaru, A.E., Holmes, D.E., Franks, A.E., Orellana, R., Risso, C., Nevin, K.P., 2011. Geobacter. The microbe electric's physiology, ecology, and practical applications. In: Adv. Microb. Physiol. Academic Press, pp. 1–100. https://doi.org/10.1016/B978-0-12-387661-4.00004-5.

Luther, R., 2017. Lubricants in the environment. In: Lubr. Lubr. Wiley-VCH Verlag GmbH & Co. KGaA, Weinheim, Germany, pp. 153–236. https://doi.org/10.1002/9783527645565.ch7.

Malina, G., Zawierucha, I., 2007. Potential of bioaugmentation and biostimulation for enhancing intrinsic biodegradation in oil hydrocarbon-contaminated soil. Bioremediat. J. 11, 141–147. https://doi.org/10.1080/10889860701548648.

Mang, T., Gosalia, A., 2017. Lubricants and their market. In: Lubr. Lubr. Wiley-VCH Verlag GmbH & Co. KGaA, Weinheim, Germany, pp. 1–10. https://doi.org/10.1002/9783527645565.ch1.

Marti, R., Bécouze-Lareure, C., Ribun, S., Marjolet, L., Bernardin Souibgui, C., Aubin, J. B., Lipeme Kouyi, G., Wiest, L., Blaha, D., Cournoyer, B., 2017. Bacteriome genetic structures of urban deposits are indicative of their origin and impacted by chemical pollutants. Sci. Rep. 7, 1–14. https://doi.org/10.1038/s41598-017-13594-8.

Mezősi, G., 2017. Soils of Hungary. Springer, Cham, pp. 165–174. https://doi.org/10.1007/978-3-319-45183-1_4.

Militon, C., Boucher, D., Vachelard, C., Perchet, G., Barra, V., Troquet, J., Peyretaillade, E., Peyret, P., 2010. Bacterial community changes during bioremediation of aliphatic hydrocarbon-contaminated soil. FEMS Microbiol. Ecol. 74, 669–681. https://doi.org/10.1111/j.1574-6941.2010.00982.x.

Montagnolli, R.N., Lopes, P.R.M., Bidoia, E.D., 2015. Screening the toxicity and biodegradability of petroleum hydrocarbons by a rapid colorimetric method. Arch. Environ. Contam. Toxicol. 68, 342–353. https://doi.org/10.1007/s00244-014-0112-9.

Nair, P.M.G., Chung, I.M., 2017. Evaluation of stress effects of copper oxide nanoparticles in Brassica napus L. seedlings. 3 Biotech 7, 1–8. https://doi.org/10.1007/s13205-017-0929-9.

Nowak, P., Kucharska, K., Kamiński, M., 2019. Ecological and health effects of lubricant oils emitted into the environment. IJERPH 16, 3002. https://doi.org/10.3390/ijerph16163002.

Nwankwegu, A.S., Orji, M.U., Onwosi, C.O., 2016. Studies on organic and in-organic biostimulants in bioremediation of diesel-contaminated arable soil. Chemosphere 162, 148–156. https://doi.org/10.1016/j.chemosphere.2016.07.074.

Ogbo, E., 2009. Effects of diesel fuel contamination on seed germination of four crop plants - Arachis hypogaea, Vigna unguiculata, Sorghum bicolor and Zea mays. Afr. J. Biotechnol. 8 https://doi.org/10.4314/AJB.V8I2.59777.

Oliver, J.D., 2010. Recent findings on the viable but nonculturable state in pathogenic bacteria. FEMS Microbiol. Rev. 34, 415–425. https://doi.org/10.1111/j.1574-6976.2009.00200.x.
Ossai, I.C., Ahmed, A., Hassan, A., Hamid, F.S., 2020. Remediation of soil and water contaminated with petroleum hydrocarbon: a review. Environ. Technol. Innov. 17, 100526 https://doi.org/10.1016/j.eti.2019.100526.
Pacwa-Płociniczak, M., Biniecka, P., Bondarczuk, K., Piotrowska-Seget, Z., 2020. Metagenomic functional profiling reveals differences in bacterial composition and function during bioaugmentation of aged petroleum-contaminated soil. Front. Microbiol. 11, 2106. https://doi.org/10.3389/fmicb.2020.02106.
Pacwa-Płociniczak, M., Czapla, J., Płociniczak, T., Piotrowska-Seget, Z., 2019. The effect of bioaugmentation of petroleum-contaminated soil with Rhodococcus erythropolis strains on removal of petroleum from soil. Ecotoxicol. Environ. Saf. 169, 615–622. https://doi.org/10.1016/J.ECOENV.2018.11.081.
Pedregosa, F., Grisel, O., Weiss, R., Passos, A., Brucher, M., Varoquax, G., Gramfort, A., Michel, V., Thirion, B., Grisel, O., Blondel, M., Prettenhofer, P., Weiss, R., Dubourg, V., Brucher, M., 2011. Scikit-learn: machine learning in Python. J. Mach. Learn. Res. 12, 2825–2830.
Peng, C., Tang, Y., Yang, H., He, Y., Liu, Y., Liu, D., Qian, Y., Lu, L., 2020. Time- and compound-dependent microbial community compositions and oil hydrocarbon degrading activities in seawater near the Chinese Zhoushan Archipelago. Mar. Pollut. Bull. 152, 110907 https://doi.org/10.1016/j.marpolbul.2020.110907.
Pinheiro, C.T., Ascensão, V.R., Cardoso, C.M., Quina, M.J., Gando-Ferreira, L.M., 2017a. An overview of waste lubricant oil management system: physicochemical characterization contribution for its improvement. J. Clean. Prod. 150, 301–308. https://doi.org/10.1016/J.JCLEPRO.2017.03.024.
Pinheiro, C.T., Rendall, R., Quina, M.J., Reis, M.S., Gando-Ferreira, L.M., 2017b. Assessment and prediction of lubricant oil properties using infrared spectroscopy and advanced predictive analytics. Energy Fuels 31, 179–187. https://doi.org/10.1021/acs.energyfuels.6b01958.
Poi, G., Aburto-Medina, A., Mok, P.C., Ball, A.S., Shahsavari, E., 2017. Large scale bioaugmentation of soil contaminated with petroleum hydrocarbons using a mixed microbial consortium. Ecol. Eng. 102, 64–71. https://doi.org/10.1016/j.ecoleng.2017.01.048.
Prince, R.C., Amande, T.J., McGenity, T.J., 2018. Prokaryotic hydrocarbon degraders. In: Taxon. Genomics Ecophysiol. Hydrocarb. Microbes. Springer International Publishing, pp. 1–41. https://doi.org/10.1007/978-3-319-60053-6_15-1.
Quast, C., Pruesse, E., Yilmaz, P., Gerken, J., Schweer, T., Yarza, P., Peplies, J., Glöckner, F.O., 2013. The SILVA ribosomal RNA gene database project: Improved data processing and web-based tools. Nucleic Acids Res. 41, D590–D596. https://doi.org/10.1093/nar/gks1219.
Rognes, T., Flouri, T., Nichols, B., Quince, C., Mahé, F., 2016. VSEARCH: a versatile open source tool for metagenomics. PeerJ 4, 2584. https://doi.org/10.7717/peerj.2584.
Ryan, R.P., Monchy, S., Cardinale, M., Taghavi, S., Crossman, L., Avison, M.B., Berg, G., van der Lelie, D., Dow, J.M., 2009. The versatility and adaptation of bacteria from the genus Stenotrophomonas. Nat. Rev. Microbiol. 7, 514–525. https://doi.org/10.1038/nrmicro2163.
Sales da Silva, I.G., Gomes de Almeida, F.C., Padilha da Rocha e Silva, N.M., Casazza, A. A., Converti, A., Asfora Sarubbo, L., 2020. Soil bioremediation: overview of technologies and trends. Energies 13, 4664. https://doi.org/10.3390/en13184664.
Sheremet, A., Jones, G.M., Jarett, J., Bowers, R.M., Bedard, I., Culham, C., Eloe-Fadrosh, E.A., Ivanova, N., Malmstrom, R.R., Grasby, S.E., Woyke, T., Dunfield, P.F., 2020. Ecological and genomic analyses of candidate phylum WPS-2 bacteria in an unvegetated soil. Environ. Microbiol. 22, 3143–3157. https://doi.org/10.1111/1462-2920.15054.
Silva, N.M., de Oliveira, A.M.S.A., Pegorin, S., Giusti, C.E., Ferrari, V.B., Barbosa, D., Martins, L.F., Morais, C., Setubal, J.C., Vasconcellos, S.P., da Silva, A.M., de Oliveira, J.C.F., Pascon, R.C., Viana-Niero, C., 2019. Characterization of novel hydrocarbon-degrading Gordonia paraffinivorans and Gordonia sihwensis strains isolated from composting. PLoS One 14, 0215396. https://doi.org/10.1371/journal.pone.0215396.
Singleton, D.R., Jones, M.D., Richardson, S.D., Aitken, M.D., 2013. Pyrosequence analyses of bacterial communities during simulated in situ bioremediation of polycyclic aromatic hydrocarbon-contaminated soil. Appl. Microbiol. Biotechnol. 97, 8381–8391. https://doi.org/10.1007/s00253-012-4531-0.
Stepniewska, Z., Wolińska, A., Ziomek, J., 2009. Response of soil catalase activity to chromium contamination. J. Environ. Sci. 21, 1142–1147. https://doi.org/10.1016/S1001-0742(08)62394-3.
Su, X., Xue, B., Wang, Y., Hashmi, M.Z., Lin, H., Chen, J., Mei, R., Wang, Z., Sun, F., 2019c. Bacterial community shifts evaluation in the sediments of Puyang River and its nitrogen removal capabilities exploration by resuscitation promoting factor. Ecotoxicol. Environ. Saf. 179, 188–197. https://doi.org/10.1016/J.ECOENV.2019.04.067.
Suja, F., Rahim, F., Taha, M.R., Hambali, N., Rizal Razali, M., Khalid, A., Hamzah, A., 2014. Effects of local microbial bioaugmentation and biostimulation on the bioremediation of total petroleum hydrocarbons (TPH) in crude oil contaminated soil based on laboratory and field observations. Int. Biodeterior. Biodegrad. 90, 115–122. https://doi.org/10.1016/J.IBIOD.2014.03.006.
Sun, G.D., Xu, Y., Liu, Y., Liu, Z.P., 2014. Microbial community dynamics of soil mesocosms using Orychophragmus violaceus combined with Rhodococcus ruber Em1 for bioremediation of highly PAH-contaminated soil. Appl. Microbiol. Biotechnol. 98, 10243–10253. https://doi.org/10.1007/s00253-014-5971-5.
Su, X.M., Liu, Y.D., Hashmi, M.Z., Ding, L.X., Shen, C.F., 2015c. Culture-dependent and culture-independent characterization of potentially functional biphenyl-degrading bacterial community in response to extracellular organic matter from Micrococcus luteus. Microb. Biotechnol. 8, 569–578. https://doi.org/10.1111/1751-7915.12266.
Su, X., Li, S., Cai, J., Xiao, Y., Tao, L., Hashmi, M.Z., Lin, H., Chen, J., Mei, R., Sun, F., 2019a. Aerobic degradation of 3,3′,4,4′-tetrachlorobiphenyl by a resuscitated strain Castellaniella sp. SPC4: Kinetics model and pathway for biodegradation. Sci. Total Environ. 688, 917–925. https://doi.org/10.1016/J.SCITOTENV.2019.06.364.
Su, X., Li, S., Xie, M., Tao, L., Zhou, Y., Xiao, Y., Lin, H., Chen, J., Sun, F., 2021. Enhancement of polychlorinated biphenyl biodegradation by resuscitation promoting factor (Rpf) and Rpf-responsive bacterial community. Chemosphere 263, 128283. https://doi.org/10.1016/j.chemosphere.2020.128283.
Su, X., Liu, Y., Hashmi, M.Z., Hu, J., Ding, L., Wu, M., Shen, C., 2015a. Rhodococcus biphenylivorans sp. nov., a polychlorinated biphenyl-degrading bacterium, Antonie van Leeuwenhoek. Int. J. Gen. Mol. Microbiol. 107, 55–63. https://doi.org/10.1007/s10482-014-0303-4.
Su, X., Shen, H., Yao, X., Ding, L., Yu, C., Shen, C., 2013. A novel approach to stimulate the biphenyl-degrading potential of bacterial community from PCBs-contaminated soil of e-waste recycling sites. Bioresour. Technol. 146, 27–34. https://doi.org/10.1016/j.biortech.2013.07.028.
Su, X., Sun, F., Wang, Y., Hashmi, M.Z., Guo, L., Ding, L., Shen, C., 2015b. Identification, characterization and molecular analysis of the viable but nonculturable Rhodococcus biphenylivorans. Sci. Rep. 5, 18590. https://doi.org/10.1038/srep18590.
Su, X., Wang, Y., Xue, B., Hashmi, M.Z., Lin, H., Chen, J., Wang, Z., Mei, R., Sun, F., 2019b. Impact of resuscitation promoting factor (Rpf) in membrane bioreactor treating high-saline phenolic wastewater: performance robustness and Rpf-responsive bacterial populations. Chem. Eng. J. 357, 715–723. https://doi.org/10.1016/J.CEJ.2018.09.197.
Tischer, K., Kleinsteuber, S., Schleinitz, K.M., Fetzer, I., Spott, O., Stange, F., Lohse, U., Franz, J., Neumann, F., Gerling, S., Schmidt, C., Hasselwander, E., Harms, H., Wendeberg, A., 2013. Microbial communities along biogeochemical gradients in a hydrocarbon-contaminated aquifer. Environ. Microbiol. 15, 2603–2615. https://doi.org/10.1111/1462-2920.12168.
Tsuboi, S., Yamamura, S., Nakajima-Kambe, T., Iwasaki, K., 2015. Diversity of alkane hydroxylase genes on the rhizoplane of grasses planted in petroleum-contaminated soils. Springerplus 4, 526. https://doi.org/10.1186/s40064-015-1312-0.
Uribe-Flores, M.M., Cerqueda-García, D., Hernández-Nuñez, E., Cadena, S., García-Cruz, N.U., Trejo-Hernández, M.R., Aguirre-Macedo, M.L., García-Maldonado, J.Q., 2019. Bacterial succession and co-occurrence patterns of an enriched marine microbial community during light crude oil degradation in a batch reactor. J. Appl. Microbiol. 127, 495–507. https://doi.org/10.1111/jam.14307.
Varjani, S.J., Upasani, V.N., 2017. Critical review on biosurfactant analysis, purification and characterization using rhamnolipid as a model biosurfactant. Bioresour. Technol. 232, 389–397. https://doi.org/10.1016/j.biortech.2017.02.047.
Varon, M., Shilo, M., 1981. Inhibition of the predatory activity of Bdellovibrio by various environmental pollutants. Microb. Ecol. 7, 107–111. https://doi.org/10.1007/BF02032492.
Wang, S.-Y., Kuo, Y.-C., Hong, A., Chang, Y.-M., Kao, C.-M., 2016. Bioremediation of diesel and lubricant oil-contaminated soils using enhanced landfarming system. Chemosphere 164, 558–567. https://doi.org/10.1016/J.CHEMOSPHERE.2016.08.128.
Wang, C.C., Li, C.H., Yang, C.F., 2019. Acclimated methanotrophic consortia for aerobic co-metabolism of trichloroethene with methane. Int. Biodeterior. Biodegrad. 142, 52–57. https://doi.org/10.1016/j.ibiod.2019.05.002.
Ward, L.M., Cardona, T., Holland-Moritz, H., 2019. Evolutionary implications of anoxygenic phototrophy in the bacterial phylum candidatus eremiobacterota (WPS-2). Front. Microbiol. 10, 1658. https://doi.org/10.3389/fmicb.2019.01658.
Wei, Z., Wang, J.J., Gaston, L.A., Li, J., Fultz, L.M., DeLaune, R.D., Dodla, S.K., 2020. Remediation of crude oil-contaminated coastal marsh soil: Integrated effect of biochar, rhamnolipid biosurfactant and nitrogen application. J. Hazard. Mater. 396, 122595 https://doi.org/10.1016/j.jhazmat.2020.122595.
Willems, A., 2014. The family Comamonadaceae. In: The Prokaryotes: Alphaproteobacteria and Betaproteobacteria. Springer-Verlag, Berlin Heidelberg, pp. 777–851. https://doi.org/10.1007/978-3-642-30197-1_238.
Wolińska, A., Kuźniar, A., Szafranek-Nakonieczna, A., Jastrzębska, N., Roguska, E., Stępniewska, Z., 2016. Biological activity of autochthonic bacterial community in oil-contaminated soil. Water Air Soil Pollut. 227, 1–12. https://doi.org/10.1007/s11270-016-2825-z.
Wu, M., Dick, W.A., Li, W., Wang, X., Yang, Q., Wang, T., Xu, L., Zhang, M., Chen, L., 2016. Bioaugmentation and biostimulation of hydrocarbon degradation and the microbial community in a petroleum-contaminated soil. Int. Biodeterior. Biodegrad. 107, 158–164. https://doi.org/10.1016/J.IBIOD.2015.11.019.
Wu, M., Guo, X., Wu, J., Chen, K., 2020. Effect of compost amendment and bioaugmentation on PAH degradation and microbial community shifting in petroleum-contaminated soil. Chemosphere 256, 126998. https://doi.org/10.1016/j.chemosphere.2020.126998.
Wu, M., Ye, X., Chen, K., Li, W., Yuan, J., Jiang, X., 2017. Bacterial community shift and hydrocarbon transformation during bioremediation of short-term petroleum-contaminated soil. Environ. Pollut. 223, 657–664. https://doi.org/10.1016/j.envpol.2017.01.079.
Xu, X., Liu, W., Tian, S., Wang, W., Qi, Q., Jiang, P., Gao, X., Li, F., Li, H., Yu, H., 2018. Petroleum hydrocarbon-degrading bacteria for the remediation of oil pollution under aerobic conditions: a perspective analysis. Front. Microbiol. 9, 2885. https://doi.org/10.3389/fmicb.2018.02885.
Yadav, N., Yadav, A.N., 2019. Biodegradation of biphenyl compounds by soil microbiomes. Biodivers. Int. J. 3, 37–40. https://doi.org/10.15406/bij.2019.03.00125.
Yang, S., Wen, X., Zhao, L., Shi, Y., Jin, H., 2014. Crude oil treatment leads to shift of bacterial communities in soils from the deep active layer and upper permafrost along

the China-Russia crude oil pipeline route. PLoS One 9, 96552. https://doi.org/10.1371/journal.pone.0096552.

Ye, Z., Li, H., Jia, Y., Fan, J., Wan, J., Guo, L., Su, X., Zhang, Y., Wu, W.M., Shen, C., 2020. Supplementing resuscitation-promoting factor (Rpf) enhanced biodegradation of polychlorinated biphenyls (PCBs) by Rhodococcus biphenylivorans strain TG9T. Environ. Pollut. 263, 114488 https://doi.org/10.1016/j.envpol.2020.114488.

Yu, C., Liu, Y., Jia, Y., Su, X., Lu, L., Ding, L., Shen, C., 2020. Extracellular organic matter from Micrococcus luteus containing resuscitation-promoting factor in sequencing batch reactor for effective nutrient and phenol removal. Sci. Total Environ. 727, 138627 https://doi.org/10.1016/j.scitotenv.2020.138627.

Zheng, W., Tsompana, M., Ruscitto, A., Sharma, A., Genco, R., Sun, Y., Buck, M.J., 2015. An accurate and efficient experimental approach for characterization of the complex oral microbiota. Microbiome 3, 48. https://doi.org/10.1186/s40168-015-0110-9.

Zheng, J., Wang, S., Zhou, A., Zhao, B., Dong, J., Zhao, X., Li, P., Yue, X., 2020. Efficient elimination of sulfadiazine in an anaerobic denitrifying circumstance: biodegradation characteristics, biotoxicity removal and microbial community analysis. Chemosphere 252, 126472. https://doi.org/10.1016/j.chemosphere.2020.126472.

Ławniczak, Ł., Woźniak-Karczewska, M., Loibner, A.P., Heipieper, H.J., Chrzanowski, Ł., 2020. Microbial degradation of hydrocarbons—basic principles for bioremediation: a review. Molecule 25, 856. https://doi.org/10.3390/MOLECULES25040856.